

Collinear Factorization for Single Transverse-Spin Asymmetry in Drell-Yan Processes

J.P. Ma^{1,2}, H.Z. Sang³ and S.J. Zhu¹

¹ *Institute of Theoretical Physics, Academia Sinica, P.O. Box 2735, Beijing 100190, China*

² *Center for High-Energy Physics, Peking University, Beijing 100871, China*

³ *Institute of Modern Physics, School of Science, East China University of Science and Technology, 130 Meilong Road, Shanghai 200237, P.R. China*

Abstract

We study the scattering of a single parton state with a multi-parton state to derive the complete results of perturbative coefficient functions at leading order, which appear in the collinear factorization for Single transverse-Spin Asymmetry(SSA) in Drell-Yan processes with a transversely polarized hadron in the initial state. We find that the factorization formula of SSA contains hard-pole-, soft-quark-pole- and soft-gluon-pole contributions. It is interesting to note that the leading order perturbative coefficient functions of soft-quark-pole- and soft-gluon-pole contributions are extracted from parton scattering amplitudes at one-loop, while the functions of hard-pole contributions are extracted from the tree level amplitudes at tree-level. Our method to derive the factorization of SSA is different than the existing one in literature. A comparison of our results with those obtained by other method is made.

1. Introduction

In scattering processes with a transversely polarized hadron in the initial state, Single transverse-Spin Asymmetry(SSA) relative to the spin direction can be nonzero. SSA has been observed in various experiments, a review about the phenomenologies can be found in [1]. Theoretically, SSA can be predicted with the concept of QCD factorization, if large momentum transfers are large. In the factorization of SSA nonperturbative effects of the transversely polarized hadron are factorized into matrix elements of the hadron. Therefore, it will provide a new way to study the inner-structure of hadron by studying SSA. In this work we study the collinear factorization of SSA in Drell-Yan processes.

From general principles SSA can be generated if the strong interaction changes the helicities of hadrons in a scattering and the scattering amplitude has an absorptive part. In the scattering involving a transversely polarized heavy quark, the helicity of which is not conserved in QCD because of the heavy mass. The related SSA can be calculated with perturbative theory of QCD, e.g., in [2, 3]. For light hadrons in high energy processes, one can neglect the mass of light quarks. The helicity of a massless quark is conserved in QCD. But this does not mean that the helicity of a light hadron is conserved in QCD, because a light hadron is a bound state of light quarks and gluons and the helicity of a light hadron is not only a sum of helicities of light quarks.

The collinear factorization for describing SSA has been proposed in [4, 5]. With the collinear factorization SSA in various processes has been studied in [6, 7, 8, 9, 10, 11, 12, 13]. In such a factorization, the nonperturbative effects of the transversely polarized hadron are factorized into twist-3 matrix elements, or called ETQS matrix elements. Taking Drell-Yan processes as an example, SSA is factorized as a

convolution of three parts: The first part is the standard parton distribution function of the unpolarized hadron defined with twist-2 operators. The second part consists of matrix elements of the polarized hadron defined with twist-3 operators. The third part consists of perturbative coefficient functions describing the hard scattering of partons. If the factorization can be proven, the coefficient functions are free from any soft divergence like collinear- and I.R. divergence. In this approach the effects of helicity-flip are parameterized with twist-3 matrix elements, while the absorptive part of the scattering amplitude is generated in the hard scattering of partons.

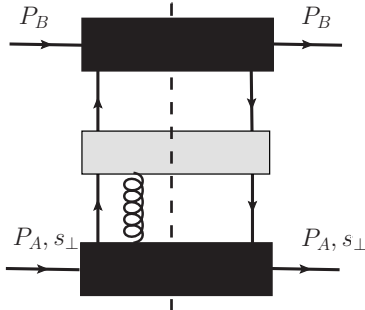


Figure 1: The cut diagram for the differential cross section of hadron scattering where the lower hadron is transversely polarized. The broken line is the cut. The black boxes represent parton density matrices of corresponding hadrons, the gray box is the forward scattering amplitude of partons.

A widely used method to derive the factorization of SSA at the leading order of α_s is the diagram expansion at hadron level. All existing results are derived with the method except those in [14, 15, 16, 17]. This method has been also used for analyzing higher-twist effects, e.g., in [18, 19]. We take the Drell-Yan process $h_A + h_B \rightarrow \ell^+ \ell^- + X$ as an example to illustrate the method. In the process h_A is transversely polarized with the spin vector s_\perp . The spin-dependent part of the differential cross section can be given by Fig.1. In Fig.1., the gray box represents Feynman diagrams for various contributions of forward parton-scattering with the cut. The lower black box represents the density matrix of the polarized hadron defined with quark- and gluon fields, and the upper black box represents the quark density matrix of the unpolarized hadron. The three parts are connected with parton lines. A collinear expansion of the momenta carried by the parton lines is performed to pick up the leading power contributions. For the partons from h_A the momentum is expanded around P_A , while the expansion for the partons from h_B is around P_B . After the expansion, one obtains an approximated form of density matrices parameterized with various nonperturbative functions, i.e., parton distributions functions and twist-3 matrix elements, and the perturbative coefficient functions of the factorization. It is interesting to note that SSA in the factorization contains not only the so-called hard-pole contributions in which all three partons from h_A carry nonzero momentum fraction, but also the so-called soft-pole contributions in which one of the three partons can have zero momentum fraction.

It should be noted that QCD factorizations, if they are proven, are general properties of QCD. These factorizations hold not only at hadron level but also when one replaces the hadron states with parton states. The perturbatively calculable parts in factorizations, i.e., the perturbative coefficient functions, do not depend on hadrons and are completely determined by the scattering of partons. To derive the factorization of SSA, one can replace hadrons with parton states and calculate SSA perturbatively. The relevant twist-2 and twist-3 matrix elements can also be calculated with the parton states. In general the obtained results will contain soft divergences which usually appear beyond leading order. By writing SSA

as a convolution of these matrix elements and perturbative coefficient functions, one can determine the functions. In this work we will take this approach to derive at leading order all perturbative coefficient functions appearing in the collinear factorization of SSA in Drell-Yan processes.

We notice that the approach taken here has been used to study factorizations only involving twist-2 operators. Applying the approach for SSA, i.e., factorizations with twist-3 operators, will provide an alternative way to derive the factorization or to calculate perturbative coefficient functions. This will also give an independent verification of results derived with other approaches. It is not the intention here to prove the factorization or that the perturbative coefficient functions are free from soft divergences at any order. This is beyond the scope of the present work. However, as we will see, we already have at leading order some perturbative coefficient functions obtained by subtraction of collinear divergences with twist-3 matrix elements, in contrast to the case only with twist-2 operators.

For the factorization only involve twist-2 operators, e.g., for the unpolarized differential cross-section one can simply replace each hadron state with a single parton state to derive the factorization. But for SSA, because of the helicity conservation of QCD it is not possible to obtain nonzero SSA and the relevant twist-3 matrix elements by replacing the transversely polarized hadron with a single quark state. But, one can construct multi-parton states to replace the polarized hadron. With the multi-parton states SSA and relevant twist-3 matrix elements are nonzero, because the helicity-flip effects can be generated through correlations between these partons.

In [14, 15] we have used multi-parton states to study the factorization. We have found [14] that with tree-level results of SSA and twist-3 matrix elements there are only the hard-pole contributions. Later, in [15] it has been realized that there is a special class of one-loop contributions to SSA which can not be factorized as one-loop corrections to the hard-pole contributions at tree-level. These one-loop contributions can only be factorized with some special twist-3 matrix elements at one-loop. These contributions are just the so-called soft-pole contributions. Their perturbative functions, although extracted from parton scattering amplitudes at one-loop, are at the same order as the hard-pole contributions derived from tree-level amplitudes.

In this work we will use multi-parton states to derive all contributions in the factorization formula for SSA in Drell-Yan processes. They are Hard-Pole(HP) contributions, Soft-Quark-Pole(SQP) contributions and Soft-Gluon-Pole(SGP) contributions. There are two types of SGP contributions. One is from the case as given in Fig.1, where the gluon from the polarized hadron has zero momentum fraction. Another is from the case where three gluons are from the polarized hadron and one of them carries zero momentum. The twist-3 matrix elements for the three gluon case have been defined in [20].

It should be mentioned that besides the collinear factorization, there is another factorization for SSA in limited regions of kinematics. If the transverse momentum of the lepton pair is small, one can use the Transverse-Momentum-Dependent(TMD) factorization. The TMD factorization for unpolarized cases have been studied in [23, 24, 25, 26, 27]. For SSA nonperturbative effects of the polarized hadron are factorized into Sivers function[21]. The properties of Sivers function and SSA with it have been studied extensively [28, 29, 30, 31, 32, 33, 34, 35, 36, 37]. In [14, 16, 17] we have also examined the TMD factorization of SSA with parton states and found an agreement with existing results.

Our work is organized as the following: In Sect.2 we give our notations for Drell-Yan processes and the definitions of relevant twist-3 matrix elements. In Sect.3 we introduce our multi-parton states. With these states one can define corresponding spin-density matrices in helicity space. The non-diagonal parts of the matrices are relevant for calculating SSA and twist-3 matrix elements. In Sect.4 we study SSA in the scattering of multi-parton state at tree-level. With tree-level results we can derive HP contributions. In Sect.5 and Sect.6 we consider SSA at one-loop level. We find a special class of one-loop contributions which give the SQP- and SGP contributions. Sect.7 is our summary.

2. SSA in Drell-Yan Processes and Definitions of Twist-3 Matrix Elements

We will use the light-cone coordinate system, in which a vector a^μ is expressed as $a^\mu = (a^+, a^-, \vec{a}_\perp) = ((a^0 + a^3)/\sqrt{2}, (a^0 - a^3)/\sqrt{2}, a^1, a^2)$ and $a_\perp^2 = (a^1)^2 + (a^2)^2$. Other notations are:

$$g_\perp^{\mu\nu} = g^{\mu\nu} - n^\mu l^\nu - n^\nu l^\mu, \quad \epsilon_\perp^{\mu\nu} = \epsilon^{\alpha\beta\mu\nu} l_\alpha n_\beta, \quad \epsilon^{\alpha\beta\mu\nu} = -\epsilon_{\alpha\beta\mu\nu}, \quad \epsilon^{0123} = 1 \quad (1)$$

with the light-cone vectors l and n defined as $l^\mu = (1, 0, 0, 0)$ and $n^\mu = (0, 1, 0, 0)$, respectively. We consider the Drell-Yan process:

$$h_A(P_A, s) + h_B(P_B) \rightarrow \gamma^*(q) + X \rightarrow \ell^- + \ell^+ + X, \quad (2)$$

where h_A is a spin-1/2 hadron with the spin-vector s . We take a light-cone coordinate system in which the momenta and the spin are :

$$P_A^\mu \approx (P_A^+, 0, 0, 0), \quad P_B^\mu \approx (0, P_B^-, 0, 0), \quad s^\mu = (0, 0, \vec{s}_\perp). \quad (3)$$

The mass of hadrons are neglected. The spin of h_B is averaged. The invariant mass of the observed lepton pair is $Q^2 = q^2$. We are interested in the spin-dependent part of the differential cross section, which can be written as:

$$\frac{d\sigma}{d^2q_\perp dq^+ dq^-}(\vec{s}_\perp) - \frac{d\sigma}{d^2q_\perp dq^+ dq^-}(-\vec{s}_\perp) = \frac{8\pi\alpha_{em}^2}{3SQ^2} \epsilon_\perp^{\alpha\beta} s_{\perp\alpha} q_{\perp\beta} \mathcal{W}_T, \quad (4)$$

in which $S = 2P_A^+ P_B^-$. We parameterize the momentum of the lepton pair as:

$$q^\mu = (xP_A^+, yP_B^-, \vec{q}_\perp). \quad (5)$$

The structure function $\mathcal{W}_T(x, y, q_\perp)$ is related to the spin dependent part of the hadronic tensor

$$W^{\mu\nu} = \sum_X \int \frac{d^4x}{(2\pi)^4} e^{iq \cdot x} \langle h_A(P_A, s_\perp), h_B(P_B) | \bar{q}(0) \gamma^\nu q(0) | X \rangle \langle X | \bar{q}(x) \gamma^\mu q(x) | h_B(P_B), h_A(P_A, s_\perp) \rangle, \quad (6)$$

by:

$$\left(-g_{\mu\nu} + \frac{q_\mu q_\nu}{q^2} \right) W^{\mu\nu} = \epsilon_\perp^{\alpha\beta} s_{\perp\alpha} q_{\perp\beta} \mathcal{W}_T + \dots, \quad (7)$$

where \dots stand for spin-independent part.

For large Q^2 the structure function \mathcal{W}_T can be factorized in the form of a convolution of perturbative functions with the standard parton distribution functions of h_B and twist-3 matrix elements of h_A . The definitions of standard parton distribution functions with twist-2 operators can be found in literature. Here we discuss the definitions of twist-3 matrix elements of the transversely polarized hadron. The quark-gluon twist-3 matrix elements have been introduced in [4, 5] firstly. We take a variant form and define them in the light-cone gauge $n \cdot G = 0$:

$$\begin{aligned} T_{q^+}(x_1, x_2) &= s_{\perp\mu} \int \frac{dy_1 dy_2}{4\pi} e^{-iy_2(x_2-x_1)P^+ - iy_1 x_1 P^+} \langle P, \vec{s}_\perp | \bar{\psi}(y_1 n) \\ &\quad \cdot \gamma^+ \left(\tilde{G}^{+\mu}(y_2 n) + i\gamma_5 G^{+\mu}(y_2 n) \right) \psi(0) | P, \vec{s}_\perp \rangle, \\ T_{q^-}(x_1, x_2) &= s_{\perp\mu} \int \frac{dy_1 dy_2}{4\pi} e^{-iy_2(x_2-x_1)P^+ - iy_1 x_1 P^+} \langle P, \vec{s}_\perp | \bar{\psi}(y_1 n) \\ &\quad \cdot \gamma^+ \left(\tilde{G}^{+\mu}(y_2 n) - i\gamma_5 G^{+\mu}(y_2 n) \right) \psi(0) | P, \vec{s}_\perp \rangle, \end{aligned} \quad (8)$$

with $\tilde{G}^{+\mu} = \epsilon_{\perp}^{\mu\nu} G^+_{\nu}$. In other gauges gauge links along the direction n should be added to make the definitions gauge-invariant. One can also use the projection γ^+ or $\gamma^+ \gamma_5$ to defined twist-3 matrix element $T_{qF}(x_1, x_2)$ and $T_{q\Delta, F}(x_1, x_2)$, respectively, as in [4]. The relations between these twist-3 matrix elements are:

$$T_{q+}(x_1, x_2) = T_{qF}(x_1, x_2) + T_{q\Delta, F}(x_1, x_2), \quad T_{q-}(x_1, x_2) = T_{qF}(x_1, x_2) - T_{q\Delta, F}(x_1, x_2). \quad (9)$$

One can show that the function $T_{qF}(x_1, x_2)$ is symmetric in x_1 and x_2 and $T_{q\Delta, F}(x_1, x_2)$ is anti-symmetric in x_1 and x_2 .

The twist-3 matrix elements $T_{q\pm}(x_1, x_2)$ with $x_{1,2} > 0$ describe the correlation of those partons from h_A , which enter a hard scattering, e.g., the gray part of Fig.1. In the hard scattering, the initial quark carries the momentum fraction x_2 , the gluon carries the momentum fraction $x_1 - x_2$ and the final quark carries the momentum fraction x_1 . If the gluon momentum fraction is $x_1 - x_2 = 0$, the corresponding hard scattering introduces the SGP contribution to SSA. If a quark carry zero momentum, i.e., $x_1 = 0$ or $x_2 = 0$, the corresponding hard scattering introduces the SQP contribution to SSA. It is clear that the SGP contributions are related to $T_{q+}(x, x)$ with $T_{q+}(x, x) = T_{q-}(x, x) = T_{qF}(x, x)$, while the SQP contributions are related to $T_{q\pm}(0, x)$ or $T_{q\pm}(x, 0)$. There are contributions with nonzero $x_{1,2}$ and $x_1 \neq x_2$. These contributions are HP contributions. For the case $x_1 < 0$ or $x_2 < 0$ the corresponding quark fields in the definition represent antiquarks.

Instead of two quarks combined one gluon entering the hard scattering, there can be three gluons entering the hard scattering[20]. The corresponding contributions can be factorized with matrix elements defined with twist-3 gluonic operators. In this case, as we will shown, there is a leading contribution of α_s in the factorization of SSA. The contribution is a SGP contribution in which one of the three gluons carries zero momentum fraction. In general there are two types of twist-3 gluonic operators, distinguished by the color structure. One can define them in the gauge $n \cdot G = 0$:

$$\begin{aligned} O^{\alpha\beta\gamma}(x_1, x_2) &= \frac{g_s}{P^+} d^{bca} \int \frac{dy_1 dy_2}{4\pi} e^{-iy_1 x_1 P^+ - iy_2 (x_2 - x_1) P^+} \\ &\quad \langle P, s_{\perp} | G^{b,+\beta}(y_1 n) G^{c,+\gamma}(y_2 n) G^{a,+\alpha}(0) | P, s_{\perp} \rangle, \\ N^{\alpha\beta\gamma}(x_1, x_2) &= i \frac{g_s}{P^+} f^{bca} \int \frac{dy_1 dy_2}{4\pi} e^{-iy_1 x_1 P^+ - iy_2 (x_2 - x_1) P^+} \\ &\quad \langle P, s_{\perp} | G^{b,+\beta}(y_1 n) G^{c,+\gamma}(y_2 n) G^{a,+\alpha}(0) | P, s_{\perp} \rangle, \end{aligned} \quad (10)$$

There are two scalar functions can be defined for each type of color structure in the case of $x_1 = x_2 = x$ for SGP contributions:

$$\begin{aligned} O^{\alpha\beta\gamma}(x, x) &= g_{\perp}^{\alpha\beta} \tilde{s}^{\gamma} x G_{d1}(x) + [g_{\perp}^{\alpha\gamma} \tilde{s}^{\beta} + g_{\perp}^{\beta\gamma} \tilde{s}^{\alpha}] x G_{d2}(x), \\ N^{\alpha\beta\gamma}(x, x) &= g_{\perp}^{\alpha\beta} \tilde{s}^{\gamma} x G_{f1}(x) + [g_{\perp}^{\alpha\gamma} \tilde{s}^{\beta} + g_{\perp}^{\beta\gamma} \tilde{s}^{\alpha}] x G_{f2}(x). \end{aligned} \quad (11)$$

In general the function \mathcal{W}_T in the collinear factorization can be divided into four parts:

$$\mathcal{W}_T = \mathcal{W}_T \Big|_{HP} + \mathcal{W}_T \Big|_{SQP} + \mathcal{W}_T \Big|_{SGPF} + \mathcal{W}_T \Big|_{SGPG}. \quad (12)$$

For SGP contributions one can have two different contributions factorized with the quark-gluon- or purely gluonic twist-3 matrix elements, denoted by the subscriber $SGPF$ and $SGPG$ respectively. Each of the four parts can be expressed as convolutions of parton distributions, twist-3 matrix elements discussed in the above, and perturbative coefficient functions. Details of the convolutions will be given in the following sections.

The goal of our work is to derive all perturbative functions at leading order of α_s . For HP contributions at leading order we only need to calculate with parton states parton scattering amplitudes and twist-3 matrix elements at tree-level. At one-loop level, there are in general collinear divergences in \mathcal{W}_T . As observed in [15], at one-loop there is a class of contributions, whose collinear divergences can not be subtracted by using one-loop results of twist-3 matrix elements in the factorized HP contributions derived with tree-level results. These contributions hence can not be taken as one-loop corrections to the perturbative coefficient functions in HP contributions. In fact, the collinear divergences can be subtracted by the so-called soft-pole twist-3 matrix elements in which one parton carries zero momentum fraction. This is the origin of the soft-pole contributions. The soft-pole matrix elements are zero at tree-level, but nonzero at one-loop. This results in that the perturbative coefficient functions of the soft-pole contributions are at the same order of those of the HP contributions derived from tree-level.

3. Spin-Density Matrices and Multi-parton States

We consider a system $|N[\lambda]\rangle$ with total spin $1/2$. The system moves in the z -direction with the helicity $\lambda = \pm$ and can be a superposition of various multi-parton states. We consider a forward scattering of the system through some operator \mathcal{O} which do not change helicity of quarks. The operator can be those used to define twist-3 matrix elements, or the hadronic tensor. In the later, the forward scattering is with some additional particles which are unpolarized. The transition amplitude is given as:

$$\mathcal{M}_{\lambda_2\lambda_1} = \langle N[\lambda_2] | \mathcal{O} | N[\lambda_1] \rangle. \quad (13)$$

We use $\lambda_{1,2} = \pm$ to denote the helicity of the initial- and final state, respectively. The transition amplitude in the helicity space is 2×2 matrix and can be expanded as:

$$\mathcal{M}_{\lambda_2\lambda_1} = \left[a + \vec{b} \cdot \vec{\sigma} \right]_{\lambda_2\lambda_1}, \quad (14)$$

or it can also be described with a spin vector $s^\mu = (s^0, \vec{s})$:

$$\mathcal{M}(s) = \left[a + \vec{b} \cdot \vec{s} \right], \quad s^2 = -1. \quad (15)$$

From the above the transverse-spin dependent part is determined by \vec{b}_\perp , i.e., the non-diagonal part in the helicity space. SSA appears if the non-diagonal part of the hadronic tensor in Eq.(6) in the helicity space is non zero.

Because of helicity-conservation of QCD the non-diagonal part of \mathcal{M} in Eq.(14) is zero, if $|N[\lambda]\rangle$ is a single quark state. Instead of a single quark one can consider the following multi-parton state:

$$|N[\lambda]\rangle = |q[\lambda]\rangle + c_1 |qq[\lambda]\rangle + c_2 |qq\bar{q}[\lambda]\rangle + c_3 |qgg[\lambda]\rangle + \dots, \quad (16)$$

where all partons move in the z -direction, the sum of helicities of partons is $1/2$ or $-1/2$. We will give later the details about the momenta and color structure of these partons. The \dots stand for possible states with more than 3 partons. We do not need to consider the states with more than 3 partons. The reason is the following: The leading power contributions to SSA come from those parton scattering processes, in which only three partons from the polarized hadrons are involved. We call these involved partons active partons. Certainly, there can be more than three partons as active partons. The resulted contributions are power-suppressed and may be factorized with operators whose twist is larger than 3. In the leading power contributions, the three active partons can be the combinations of quarks and gluons. They are

qqg , $q\bar{q}g$ and ggg . Charge-conjugated combinations should also be included. In the case described by Fig.1. the active partons are qqg . It is clearly that with first three states in Eq.(16) one can have all combinations by taking some partons as spectators.

If we calculate the non-diagonal part of \mathcal{M} in Eq.(14) with the multi-parton state in Eq.(16), one will find with the helicity conservation of quarks nonzero contributions only from the interference between different states in the right hand side of Eq.(16). If we replace h_A with the above state and h_B with a single unpolarized parton in Eq.(6), we will also get nonzero result for the spin-dependent part of $W^{\mu\nu}$ or for \mathcal{W}_T . Similarly, the defined twist-3 matrix elements are also nonzero with the state $|N[\lambda]\rangle$. These nonzero results allow us to study the factorization of SSA.

In [16, 17] factorizations of SSA in Drell-Yan processes have been studied with the first two terms in Eq.(16) in the kinematical region $q_\perp^2/Q^2 \ll 1$. In this case, all partons are active. Non of them can be a spectator parton. But for interferences between other states, some partons can be spectators, because we only need to consider those interferences with three active partons. The existence of possible spectators only affects overall factors of interested quantities like \mathcal{W}_T and twist-3 matrix elements, it has no effect on the derivation of perturbative coefficient functions. Hence, for our purpose we only need to consider those matrix elements $\langle ab|\mathcal{O}|c\rangle$ or $\langle c|\mathcal{O}|ab\rangle$, where a, b and c are quarks or gluons. These matrix elements can be obtained from the interferences between different states in Eq.(16) by taking out some partons as spectators. We will illustrate this in the following.

For the interference between the q - and the qg -component, non of partons can be a spectator. We define the state $|q[\lambda]\rangle$ and the state $|qg[\lambda]\rangle$ as:

$$\begin{aligned} |q(p, \lambda_q)\rangle &= b_{i_c}^\dagger(p, \lambda_q)|0\rangle, & |q(p_1, \lambda_q)g(p_2, \lambda_g)\rangle &= T_{j_c i_c}^a b_{j_c}^\dagger(p_1, \lambda_q) a_a^\dagger(p_2, \lambda_g)|0\rangle, \\ p^\mu &= (p^+, 0, 0, 0), & p_1^\mu &= x_0 p^\mu, & p_2 &= (1 - x_0)p^\mu = \bar{x}_0 p^\mu, \end{aligned} \quad (17)$$

where b_i^\dagger is the quark creation operator with i as the color index, a_a^\dagger is the gluon creation operator with a as the color index. $\lambda_q(\lambda_g)$ is the helicity of the quark(gluon). To simplify the notations we will write $p^+ = P_A^+$ and $\bar{p}^- = P_B^-$. It is straightforward to obtain the non-diagonal part as

$$\begin{aligned} \mathcal{M}_{+-}^{(qg)} &= \mathcal{C}^{qg} \left[\langle q(p, +)|\mathcal{O}|q(p_1, +)g(k, -)\rangle + \langle q(p_1, -)g(k, +)|\mathcal{O}|q(p, -)\rangle \right], \\ \mathcal{M}_{-+}^{(qg)} &= \mathcal{C}^{qg} \left[\langle q(p, -)|\mathcal{O}|q(p_1, -)g(k, +)\rangle + \langle q(p_1, +)g(k, -)|\mathcal{O}|q(p, +)\rangle \right]. \end{aligned} \quad (18)$$

In the above we use the index qg to denote this type of interference contribution. We also introduce a coefficient \mathcal{C}^{qg} in the non-diagonal part of the spin-density matrix. Contributions of this type to twist-3 matrix elements and \mathcal{W}_T will be proportional to \mathcal{C}^{qg} , and will be called qg -contributions. The derived perturbative function will not depend on \mathcal{C}^{qg} .

For the contribution from the $qq\bar{q}$ -state we note that the interference with the single quark state is zero if the total helicity is changed. The interference with the qqg -state does not need to be considered because at least four partons must be active and one quark is a spectator. Hence, we only need to consider the interference with the qg -state, in which one quark is a spectator and three partons are active. In this case, the forward scattering is participated by a gluon and a $q\bar{q}$ -pair. In order to have $\Delta\lambda = \pm 1$, the total helicity λ of the $q\bar{q}$ -pair must be zero. There can be two states with $\lambda = 0$ for the $q\bar{q}$ -pair. We denote the two states as :

$$|(q\bar{q})_\pm\rangle = T_{j_c i_c}^a \left[b_{j_c}^\dagger(p_1, +) a_{i_c}^\dagger(p_2, -) \pm b_{j_c}^\dagger(p_1, -) a_{i_c}^\dagger(p_2, +) \right] |0\rangle, \quad (19)$$

and the single gluon state as $|g(\lambda_g)\rangle$. The gluon carries the same color index a and the momentum p . λ_g is the helicity. d^\dagger is the create operator for the antiquark. With these states one can construct the non-diagonal part of the spin-density matrix $\mathcal{M}^{(q\bar{q})}$ as:

$$\begin{aligned}\mathcal{M}_{+-}^{(q\bar{q})} &= \mathcal{C}_+^{q\bar{q}} \left[\langle (q\bar{q})_+ | \mathcal{O} | g(-) \rangle + \langle g(+) | \mathcal{O} | (q\bar{q})_+ \rangle \right] + \mathcal{C}_-^{q\bar{q}} \left[\langle (q\bar{q})_- | \mathcal{O} | g(-) \rangle - \langle g(+) | \mathcal{O} | (q\bar{q})_- \rangle \right], \\ \mathcal{M}_{-+}^{(q\bar{q})} &= \mathcal{C}_+^{q\bar{q}} \left[\langle (q\bar{q})_+ | \mathcal{O} | g(+) \rangle + \langle g(-) | \mathcal{O} | (q\bar{q})_+ \rangle \right] - \mathcal{C}_-^{q\bar{q}} \left[\langle (q\bar{q})_- | \mathcal{O} | g(+) \rangle - \langle g(-) | \mathcal{O} | (q\bar{q})_- \rangle \right].\end{aligned}\quad (20)$$

In the above we have introduced two coefficients $\mathcal{C}_\pm^{q\bar{q}}$ to distinguish the contributions from the two $q\bar{q}$ states. We note that there is a sign difference for the terms with $\mathcal{C}_\pm^{q\bar{q}}$ between the first and the second equation. This difference can be easily found by requiring that the state $|(q\bar{q})_-\rangle$ becomes a spin-1/2 system by adding a quark. Again, we will call all contributions from this matrix as $q\bar{q}$ -contributions. They are linear in the two coefficients $\mathcal{C}_\pm^{q\bar{q}}$. The derived perturbative functions will not depend on $\mathcal{C}_\pm^{q\bar{q}}$.

For the contribution from the qgg -state in Eq.(16), only the interference with the qg -state and with the ggg -state need to be considered here, where one quark can be taken as a spectator. In this case, one has the forward scattering as $gg \rightarrow g$ or $g \rightarrow gg$. The color of the two gluon state must be the same as the color of the one gluon state. The total helicity λ of the two gluons must be zero. There are two states with $\lambda = 0$ for a given color structure. We denote

$$|(gg)_\pm\rangle = if^{abc} \left[a_b^\dagger(p_1, +) a_c^\dagger(p_2, -) \pm a_b^\dagger(p_1, -) a_c^\dagger(p_2, +) \right] |0\rangle. \quad (21)$$

With these states one can construct the non-diagonal element of the spin-density matrix $\mathcal{M}^{(gg^F)}$ as:

$$\begin{aligned}\mathcal{M}_{+-}^{(gg^F)} &= \mathcal{F}_+^{gg} \left[\langle (gg)_+ | \mathcal{O} | g(-) \rangle + \langle g(+) | \mathcal{O} | (gg)_+ \rangle \right] - \mathcal{F}_-^{gg} \left[\langle (gg)_- | \mathcal{O} | g(-) \rangle - \langle g(+) | \mathcal{O} | (gg)_- \rangle \right], \\ \mathcal{M}_{-+}^{(gg^F)} &= \mathcal{F}_+^{gg} \left[\langle (gg)_+ | \mathcal{O} | g(+) \rangle + \langle g(-) | \mathcal{O} | (gg)_+ \rangle \right] + \mathcal{F}_-^{gg} \left[\langle (gg)_- | \mathcal{O} | g(+) \rangle - \langle g(-) | \mathcal{O} | (gg)_- \rangle \right].\end{aligned}\quad (22)$$

In the above we introduce two coefficients \mathcal{F}_\pm^{gg} to distinguish the contributions from the two states in Eq.(21). Another spin-density matrix $\mathcal{M}^{(gg^D)}$ can be constructed in this case by replacing if^{abc} in Eq.(21) with d^{abc} , and \mathcal{F}_\pm^{gg} with \mathcal{D}_\pm^{gg} in Eq.(22). We will call all contributions from these two spin-density matrices as gg -contributions. They are linear in the four coefficients \mathcal{F}_\pm^{gg} and \mathcal{D}_\pm^{gg} .

With the constructed spin-density matrices in the above one can calculate twist-3 matrix elements and the structure functions \mathcal{W}_T by taking correspond operator \mathcal{O} . It is straightforward to obtain the twist-3 matrix elements $T_{q\pm}$ at tree-level. The results from the qg -contributions are

$$\begin{aligned}T_{q+}(x_1, x_2) &= \mathcal{C}^{qg} \pi g_s \sqrt{2x_0} (N_c^2 - 1) (x_2 - x_1) \delta(1 - x_1) \delta(x_2 - x_0) + \mathcal{O}(g_s^3), \\ T_{q-}(x_1, x_2) &= -\mathcal{C}^{qg} \pi g_s \sqrt{2x_0} (N_c^2 - 1) (x_2 - x_1) \delta(1 - x_2) \delta(x_1 - x_0) + \mathcal{O}(g_s^3).\end{aligned}\quad (23)$$

The results from the $q\bar{q}$ -contributions are

$$\begin{aligned}T_{q+}(x_1, x_2) &= \pi g_s (N_c^2 - 1) \sqrt{2x_0 \bar{x}_0} \left[\left(\mathcal{C}_+^{q\bar{q}} - \mathcal{C}_-^{q\bar{q}} \right) \delta(x_1 + \bar{x}_0) \delta(x_2 - x_0) \right. \\ &\quad \left. + \left(\mathcal{C}_+^{q\bar{q}} + \mathcal{C}_-^{q\bar{q}} \right) \delta(x_2 + \bar{x}_0) \delta(x_1 - x_0) \right] + \mathcal{O}(g_s^3), \\ T_{q-}(x_1, x_2) &= \pi g_s (N_c^2 - 1) \sqrt{2x_0 \bar{x}_0} \left[\left(\mathcal{C}_+^{q\bar{q}} + \mathcal{C}_-^{q\bar{q}} \right) \delta(x_1 + \bar{x}_0) \delta(x_2 - x_0) \right. \\ &\quad \left. + \left(\mathcal{C}_+^{q\bar{q}} - \mathcal{C}_-^{q\bar{q}} \right) \delta(x_2 + \bar{x}_0) \delta(x_1 - x_0) \right] + \mathcal{O}(g_s^3).\end{aligned}\quad (24)$$

With \mathcal{W}_T calculated in the next section at leading order, one can find the factorized form of \mathcal{W}_T in terms of $T_{q\pm}$ with the above results. This is for HP contributions. In Sect.5 and 6 we will also give the results of $T_{q\pm}(x, x)$, $T_{q\pm}(0, x)$ and these gluonic twist-3 matrix elements. These results are at order of g_s^3 and will be used to factorize the soft-pole contributions.

4. Hard-Pole Contributions

As discussed in the last section, we replace the polarized hadron h_A with the multi-parton state in Eq.(16) to calculate the non-diagonal part of the constructed spin-density matrices for \mathcal{W}_T . We replace the unpolarized hadron h_B with single-parton states. In this section we will work at tree-level.

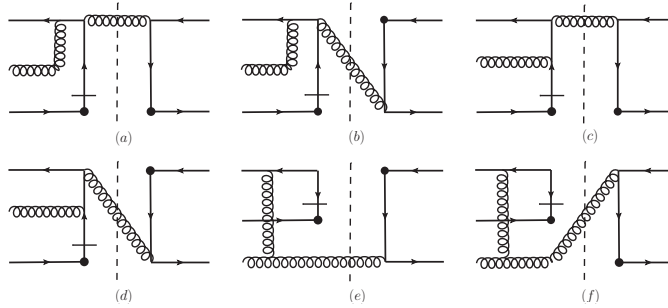


Figure 2: The diagrams for the amplitude $\bar{q} + (q + G) \rightarrow \gamma^* + X \rightarrow \bar{q} + q$ at tree-level. The black dots denote the insertion of electromagnetic current operator. Broken lines represent the cut. For the propagators with a short bar only the absorptive part of the propagator is taken into account.

We first consider the qg -contributions. If we replace h_B with an antiquark \bar{q} with the momentum $\bar{p}^\mu = (0, \bar{p}^-, 0, 0)$, the leading order contribution to \mathcal{W}_T comes from diagrams in Fig.2. The complex conjugated diagrams should be included in order to obtain the non-diagonal part of the spin-density matrix $\mathcal{M}^{(qg)}$ given in Eq.(18). In the diagrams of Fig.2. the broken line divides each diagrams into a left- and right part. Each part represents a scattering amplitude. The short bar cutting a quark propagator is in fact a physical cut of the amplitude represented by the left part. It means that only the absorptive part of the cutting propagator is taken into account:

$$\text{Abs} \left[\frac{i\gamma \cdot k_q}{k_q^2 + i\varepsilon} \right] = \pi \delta(k_q^2) \gamma \cdot k_q, \quad (25)$$

It is straightforward to calculate these diagrams and we obtain:

$$\begin{aligned} \mathcal{W}_T \Big|_{Fig.2} &= -C^{qg} e_q^2 \frac{g_s \alpha_s}{4\pi} \frac{\sqrt{2x_0}}{q_\perp^2} \frac{N_c^2 - 1}{N_c^2} \delta(\bar{x} - y\bar{x}_0) \delta(s(1-x)(1-y) - q_\perp^2) (N_c^2 + y - 1) \\ &\cdot \frac{1}{1-y} \left[y^2 + x_0 - |\lambda_q|(y^2 - x_0) \right], \end{aligned} \quad (26)$$

with $s = 2p^+\bar{p}^-$. e_q is the electric charge of the quark q in unit e . The δ -function of $1 - x - y\bar{x}_0$ is from the cutting quark propagator. The terms with $|\lambda_q| = 1$ are quark-spin dependent, because the external quark lines are extracted with $\lambda_q \gamma_5 \gamma \cdot p$.

With the qg -contributions of $T_{q\pm}$ one can write the above \mathcal{W}_T into a factorized form. The terms with $|\lambda_q| = 1$ should be factorized with $T_{q+} - T_{q-}$ or $T_{q\Delta,F}$, because $\gamma^+\gamma_5$ is used to define them. The other terms should be factorized with $(T_{q+} + T_{q-})$ or T_{qF} . With $T_{q\pm}$ in Eq.(23) we have the factorized form:

$$\mathcal{W}_T \Big|_{Fig.2} = \frac{e_q^2 \alpha_s}{\pi^2 N_c q_\perp^2} \int_x^1 \frac{dy_1}{y_1} \int_y^1 \frac{dy_2}{y_2} f_{\bar{q}}(y_2) \delta(\hat{s}(1-\xi_1)(1-\xi_2) - q_\perp^2) \cdot \left[\mathcal{H}_{q+}(\xi_1, \xi_2) T_{q+}(y_1, x_B) + \mathcal{H}_{q-}(\xi_1, \xi_2) T_{q-}(y_1, x_B) \right], \quad (27)$$

with

$$\begin{aligned} \mathcal{H}_{q+}(\xi_1, \xi_2) &= \frac{N_c^2 + \xi_2 - 1}{2N_c \xi_2 (1-\xi_1)(1-\xi_2)} (\xi_2 + \xi_1 - 1), & \mathcal{H}_{q-}(\xi_1, \xi_2) &= \frac{N_c^2 + \xi_2 - 1}{2N_c (1-\xi_1)(1-\xi_2)} \xi_2^2, \\ \xi_1 &= \frac{x}{y_1}, & \xi_2 &= \frac{y}{y_2}, & x_B &= \frac{q^2}{2q \cdot p}, & \hat{s} &= y_1 y_2 s. \end{aligned} \quad (28)$$

The function $f_{\bar{q}}(y_2)$ is the antiquark distribution function of h_B . For $h_B = \bar{q}$, we have $f_{\bar{q}}(y_2) = \delta(1-y_2) + \mathcal{O}(\alpha_s)$. It is noted that the derived perturbative coefficient functions do not depend on \mathcal{C}^{qg} . One can also replace h_B with a quark. In this case the results can be obtained by reversing the directions of quark lines in Fig.2. They can be obtained from the above results through charge-conjugation. We will give them at the end of this section by combining all parton flavors.

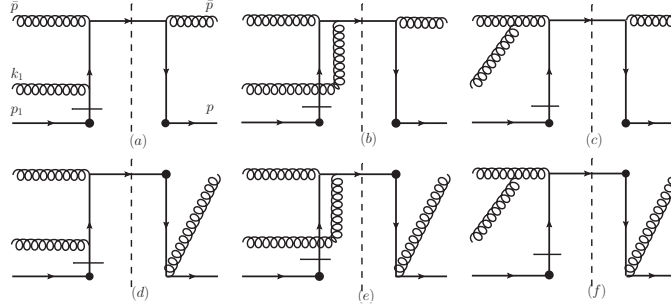


Figure 3: The diagrams for the amplitude $G + [q + G] \rightarrow \gamma^* + X \rightarrow G + q$ at tree-level

If we replace the unpolarized hadron h_B with a gluon carrying the momentum \bar{p} , the leading contributions to \mathcal{W}_T comes from Fig.3. The calculation of these diagrams is similar to the calculation of Fig.2. We have the sum of Fig.3:

$$\begin{aligned} \mathcal{W}_T \Big|_{Fig.3} &= \mathcal{C}^{qg} e_q^2 \frac{g_s \alpha_s}{4\pi N_c} \sqrt{2x_0} \delta(s(1-x)(1-y) - q_\perp^2) \delta(\bar{x} - y\bar{x}_0) \frac{1 + (y-1)N_c^2}{q_\perp^2} \\ &\cdot \left[x_0(1-y)^2 + y^2 + |\lambda_q|(x_0(1-y)^2 - y^2) \right]. \end{aligned} \quad (29)$$

This result can be factorized in the following form:

$$\mathcal{W}_T \Big|_{Fig.3} = \frac{e_q^2 \alpha_s}{\pi^2 N_c q_\perp^2} \int_x^1 \frac{dy_1}{y_1} \int_y^1 \frac{dy_2}{y_2} f_g(y_2) \delta(\hat{s}(1-\xi_1)(1-\xi_2) - q_\perp^2)$$

$$\begin{aligned}
& \cdot \left[\mathcal{H}_{g^+}(\xi_1, \xi_2) T_{q^+}(y_1, x_B) + \mathcal{H}_{g^-}(\xi_1, \xi_2) T_{q^-}(y_1, x_B) \right], \\
\mathcal{H}_{g^+}(\xi_1, \xi_2) &= \frac{1 + (\xi_2 - 1)N_c^2}{2(N_c^2 - 1)(1 - \xi_1)\xi_2} (1 - \xi_2)^2 (1 - \xi_1 - \xi_2), \\
\mathcal{H}_{g^-}(\xi_1, \xi_2) &= -\frac{1 + (\xi_2 - 1)N_c^2}{2(N_c^2 - 1)(1 - \xi_1)} \xi_2^2.
\end{aligned} \tag{30}$$

where $f_g(y_2)$ is the gluon distribution function. For $h_B = g$ we have $f_g(y) = \delta(1 - y) + \mathcal{O}(\alpha_s)$.

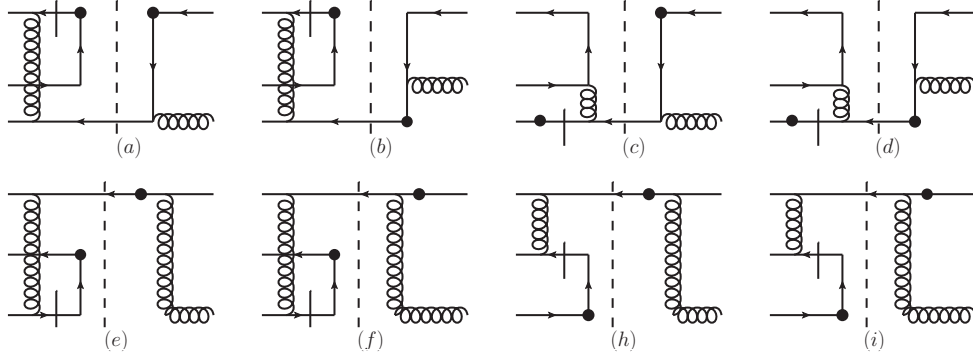


Figure 4: The diagrams for the amplitude $\bar{q} + [q + \bar{q}] \rightarrow \gamma^* + X \rightarrow \bar{q} + G$ at tree-level.

By replacing h_B with an antiquark $\bar{q}(\bar{p})$, the $q\bar{q}$ -contributions for \mathcal{W}_T are also at leading order. They are given by the diagrams in Fig.4. In the first four diagrams the anti-quark $\bar{q}(\bar{p})$ in the initial single parton state must have the same flavor as the quark in the multi-parton state, while in the last four diagrams $\bar{q}(\bar{p})$ can have different flavor. The results are:

$$\begin{aligned}
\mathcal{W}_T \Big|_{4a+4b+4c+4d} &= e_q^2 \frac{g_s \alpha_s}{2\pi q_\perp^2} \sqrt{2x_0 \bar{x}_0} \frac{N_c^2 - 1}{N_c^2} \left(\mathcal{C}_-^{q\bar{q}} + \mathcal{C}_+^{q\bar{q}}(1 - 2x_0) \right) \delta(s(1 - x)(1 - y) - q_\perp^2) \\
&\quad \cdot y \left[\frac{\delta(\bar{x} - y\bar{x}_0)}{1 - y} - (1 - y)^2 \delta(\bar{x} - yx_0) \right], \\
\mathcal{W}_T \Big|_{4e+4f+4h+4i} &= -e_q^2 \frac{g_s \alpha_s}{2\pi q_\perp^2} \sqrt{2x_0 \bar{x}_0} \frac{N_c^2 - 1}{N_c} \left(\mathcal{C}_-^{q\bar{q}} + \mathcal{C}_+^{q\bar{q}}(1 - 2x_0) \right) \delta(s(1 - x)(1 - y) - q_\perp^2) \\
&\quad \cdot \left[\delta(\bar{x} - y\bar{x}_0) + \delta(x - y\bar{x}_0) \right] (y^2 - 2y + 2).
\end{aligned} \tag{31}$$

With the tree-level results of the $q\bar{q}$ -contributions for the twist-3 matrix elements we can derive the following factorized form:

$$\begin{aligned}
\mathcal{W}_T \Big|_{4a+4b+4c+4d} &= \frac{e_q^2 \alpha_s}{\pi^2 N_c q_\perp^2} \int_x^1 \frac{dy_1}{y_1} \int_y^1 \frac{dy_2}{y_2} f_{\bar{q}}(y_2) \delta(\hat{s}(1 - \xi_1)(1 - \xi_2) - q_\perp^2) \\
&\quad \cdot \left\{ \mathcal{H}_{q\bar{q}^+}(\xi_1, \xi_2) T_{q^+}(-\hat{y}_1, x_B) + \mathcal{H}_{q\bar{q}^-}(\xi_1, \xi_2) T_{q^-}(-\hat{y}_1, x_B) \right. \\
&\quad \left. + \left[\mathcal{H}_{\bar{q}q^+}(\xi_1, \xi_2) T_{q^+}(-x_B, \hat{y}_1) + \mathcal{H}_{\bar{q}q^-}(\xi_1, \xi_2) T_{q^-}(-x_B, \hat{y}_1) \right] \right\},
\end{aligned}$$

$$\begin{aligned}
\mathcal{W}_T \Big|_{4e+4f+4h+4i} &= \frac{e_q^2 \alpha_s}{\pi^2 N_c q_\perp^2} \int_x^1 \frac{dy_1}{y_1} \int_y^1 \frac{dy_2}{y_2} f_{\bar{q}'}(y_2) \delta(\hat{s}(1-\xi_1)(1-\xi_2) - q_\perp^2) \\
&\quad \cdot \left\{ \mathcal{H}_{q\bar{q}0}(\xi_1, \xi_2) \left[T_{q+}(-\hat{y}_1, x_B) - T_{q-}(-x_B, \hat{y}_1) \right] \right. \\
&\quad \left. + \mathcal{H}_{\bar{q}q0}(\xi_1, \xi_2) \left[T_{q+}(-x_B, \hat{y}_1) - T_{q-}(-\hat{y}_1, x_B) \right] \right\}, \tag{32}
\end{aligned}$$

with $\hat{y}_1 = y_1 - x_B$ and the perturbative functions:

$$\begin{aligned}
\mathcal{H}_{q\bar{q}+}(\xi_1, \xi_2) &= \frac{1 - \xi_1 - \xi_2}{2N_c \xi_2 (1 - \xi_2)}, & \mathcal{H}_{q\bar{q}-}(\xi_1, \xi_2) &= \frac{1 - \xi_1}{2N_c \xi_2 (1 - \xi_2)}, \\
\mathcal{H}_{\bar{q}q+}(\xi_1, \xi_2) &= \frac{(1 - \xi_2)^2 (1 - \xi_1)}{2N_c \xi_2}, & \mathcal{H}_{\bar{q}q-}(\xi_1, \xi_2) &= (1 - \xi_1 - \xi_2) \frac{(1 - \xi_2)^2}{2N_c \xi_2}, \\
\mathcal{H}_{q\bar{q}0}(\xi_1, \xi_2) &= -\frac{\xi_2^2 - 2\xi_2 + 2}{2\xi_2^2} (1 - \xi_1 - \xi_2), & \mathcal{H}_{\bar{q}q0}(\xi_1, \xi_2) &= \frac{\xi_2^2 - 2\xi_2 + 2}{2\xi_2^2} (1 - \xi_1). \tag{33}
\end{aligned}$$

$f_{\bar{q}'}(y_2)$ is the antiquark distribution function for the flavor which does not need to be the same as the flavor of quarks used to calculate the twist-3 matrix element $T_{q\pm}$.

The studied contributions plus charge-conjugated processes give the all leading HP contributions for SSA. All perturbative coefficient functions are at order α_s . Combining all possible apron flavors we obtain the factorized HP contributions as:

$$\begin{aligned}
\mathcal{W}_T \Big|_{HP} &= \frac{\alpha_s}{\pi^2 N_c q_\perp^2} \int_x^1 \frac{dy_1}{y_1} \int_y^1 \frac{dy_2}{y_2} \delta(\hat{s}(1-\xi_1)(1-\xi_2) - q_\perp^2) \\
&\quad \cdot \left\{ \mathcal{H}_{q+}(\xi_1, \xi_2) \sum_{[q]} e_q^2 f_{\bar{q}}(y_2) T_{q+}(y_1, x_B) + \mathcal{H}_{q-}(\xi_1, \xi_2) \sum_{[q]} e_q^2 f_{\bar{q}}(y_2) T_{q-}(y_1, x_B) \right. \\
&\quad + \mathcal{H}_{q\bar{q}+}(\xi_1, \xi_2) \sum_{[q]} e_q^2 f_{\bar{q}}(y_2) T_{q+}(-\hat{y}_1, x_B) + \mathcal{H}_{q\bar{q}-}(\xi_1, \xi_2) \sum_{[q]} e_q^2 f_{\bar{q}}(y_2) T_{q-}(-\hat{y}_1, x_B) \\
&\quad + \mathcal{H}_{\bar{q}q+}(\xi_1, \xi_2) \sum_{[q]} e_q^2 f_{\bar{q}}(y_2) T_{q+}(-x_B, \hat{y}_1) + \mathcal{H}_{\bar{q}q-}(\xi_1, \xi_2) \sum_{[q]} e_q^2 f_{\bar{q}}(y_2) T_{q-}(-x_B, \hat{y}_1) \\
&\quad + \mathcal{H}_{q\bar{q}0}(\xi_1, \xi_2) \sum_{[q, q']} e_q^2 f_{\bar{q}'}(y_2) \left[T_{q+}(-\hat{y}_1, x_B) - T_{q-}(-x_B, \hat{y}_1) \right] \\
&\quad + \mathcal{H}_{\bar{q}q0}(\xi_1, \xi_2) \sum_{[q, q']} e_q^2 f_{\bar{q}'}(y_2) \left[T_{q+}(-x_B, \hat{y}_1) - T_{q-}(-\hat{y}_1, x_B) \right] \\
&\quad \left. + \mathcal{H}_{g+}(\xi_1, \xi_2) \sum_{[q]} e_q^2 f_g(y_2) T_{q+}(y_1, x_B) + \mathcal{H}_{g-}(\xi_1, \xi_2) \sum_{[q]} e_q^2 f_g(y_2) T_{q-}(y_1, x_B) \right\}, \tag{34}
\end{aligned}$$

where the notation for summing over flavors is defined as:

$$\begin{aligned}
\sum_{[q]} e_q^2 f_{\bar{q}}(y_2) T_{q\pm}(z_1, z_2) &= \sum_{q=u, d, s, \dots} e_q^2 \left[f_{\bar{q}}(y_2) T_{q\pm}(z_1, z_2) - f_q(y_2) T_{q\mp}(-z_2, -z_1) \right], \\
\sum_{[q, q']} e_q^2 f_{\bar{q}'}(y_2) T_{q\pm}(z_1, z_2) &= \sum_{q=u, d, s, \dots, q'=u, d, s, \dots} e_q^2 \left[f_{\bar{q}'}(y_2) T_{q\pm}(z_1, z_2) - f_{q'}(y_2) T_{q\mp}(-z_2, -z_1) \right], \\
\sum_{[q]} e_q^2 f_g(y_2) T_{q\pm}(z_1, z_2) &= \sum_{q=u, d, s, \dots} e_q^2 f_g(y_2) \left[T_{q\pm}(z_1, z_2) - T_{q\mp}(-z_2, -z_1) \right]. \tag{35}
\end{aligned}$$

It is interesting to study the limit $q_{\perp}^2/Q^2 \ll 1$ by using

$$\hat{s}\delta(\hat{s}(1-\xi_1)(1-\xi_2) - q_{\perp}^2) \approx \frac{\delta(1-\xi_1)}{(1-\xi_2)_+} + \frac{\delta(1-\xi_2)}{(1-\xi_1)_+} - \delta(1-\xi_1)\delta(1-\xi_2) \ln \frac{q_{\perp}^2}{Q^2}. \quad (36)$$

In this limit, the above contribution to \mathcal{W}_T becomes:

$$\begin{aligned} \mathcal{W}_T \Big|_{HP} &= \frac{\alpha_s}{2\pi^2(q_{\perp}^2)^2} \int_x \frac{dy_1}{y_1} \int_y \frac{dy_2}{y_2} \cdot \left\{ \frac{\delta(1-\xi_2)}{(1-\xi_1)_+} \left[\xi_1 \sum_{[q]} e_q^2 f_{\bar{q}}(y_2) T_{q^+}(y_1, x) + \sum_{[q]} e_q^2 f_{\bar{q}}(y_2) T_{q^-}(y_1, x) \right] \right. \\ &+ \delta(1-\xi_1) \left[\frac{1+\xi_2^2}{(1-\xi_2)_+} \left(1 + \frac{\xi_2-1}{N_c^2} \right) - 2\delta(1-\xi_2) \ln \frac{q_{\perp}^2}{Q^2} \right] \sum_{[q]} e_q^2 f_{\bar{q}}(y_2) T_{q^+}(y_1, y_1) \\ &+ \frac{\delta(1-\xi_1)}{N_c(N_c^2-1)} (N_c^2(1-\xi_2)-1)((1-\xi_2)^2 + \xi_2^2) \sum_{[q]} e_q^2 f_g(y_2) T_{q^+}(y_1, y_1) \\ &+ \left. \frac{\delta(1-\xi_2)}{N_c^2} \left[(1-\xi_1) \sum_{[q]} e_q^2 f_{\bar{q}}(y_2) T_{q^-}(-y_1+x, x) - \xi_1 \sum_{[q]} e_q^2 f_{\bar{q}}(y_2) T_{q^+}(-y_1+x, x) \right] \right\} \\ &\cdot \left[1 + \mathcal{O}(q_{\perp}^2/Q^2) \right]. \quad (37) \end{aligned}$$

It is noted that in the limit SGP contributions appear. If we take the limit $q_{\perp}^2/Q^2 \ll 1$ in the tree-level results for the parotnic \mathcal{W}_T 's in Eq.(26) and Eq.(29) instead of the factorized results in Eq.(27) and Eq.(30), we will not obtain the SGP contributions. However, the SGP contributions can be derived by using parotnic \mathcal{W}_T s in the limit beyond tree-level[17].

The factorized results of Fig.2 and Fig.3 have been derived in [11] with the method of the diagram expansion mentioned in the Introduction. By rewriting the above results with partonic variables which are defined as:

$$\begin{aligned} \hat{t} &= (y_1 P_A - q)^2 = -\hat{s}\xi_2(1-\xi_1) - q_{\perp}^2, & \hat{s} &= y_1 y_2 s, \\ \hat{u} &= (y_2 P_B - q)^2 = -\hat{s}\xi_1(1-\xi_2) - q_{\perp}^2, & Q^2 &= q^2 = \xi_1 \xi_2 \hat{s} - q_{\perp}^2, \end{aligned} \quad (38)$$

we find that our results agree with them in [11]. Recently, the results corresponding to the contributions from Fig.4 have been derived with the method of the diagram expansion in [8]. Again our results in Eq.(32) agree with those in [8].

5. Soft-Gluon-Pole Contributions

The SGP contributions comes from the case when one gluon with zero momentum enters hard scattering. They may come from the qg -, $q\bar{q}$ - and the gg -contributions. The qg - and $q\bar{q}$ contributions are factorized with the quark-gluon correlator $T_{q^+}(x, x) = T_{q^-}(x, x)$. Later we will show that the $q\bar{q}$ -contributions need not to be studied, because it is automatically included in the factorized form obtained from the qg -contributions. The gg -contributions are factorized with the purely gluonic correlator defined in Eq.(12). We will discuss these two types of contributions in this section separately.

5.1. The qg -Contributions

We have given the results of the qg -contributions for $T_{q_{\pm}}(x_1, x_2)$ at tree-level in Eq.(23). At this order one simply has $T_{q_{\pm}}(x, x) = 0$. However, beyond the tree-level, $T_{q_{\pm}}(x, x)$ can be nonzero. As found

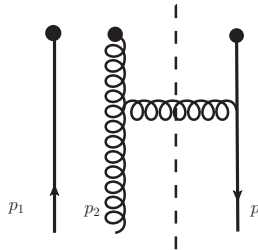


Figure 5: The diagram for $T_{q\pm}(x, x)$ at one-loop. The black dots denote the insertion of operators used to define $T_{q\pm}(x_1, x_2)$ in Eq.(8).

in [16, 17], at one-loop level there is only one diagram giving nonzero contribution to $T_{q\pm}(x, x)$ in the light-cone- or Feynman gauge. The calculation of the diagram is straightforward. The contribution has an U.V.- and a collinear divergence. Both are regularized with the dimensional regularization as poles of $\epsilon = 4 - d$. After extracting the U.V. pole we have[16, 17]:

$$T_{q\pm}(x, x, \mu) = -\mathcal{C}^{qg} \frac{g_s \alpha_s}{4} N_c (N_c^2 - 1) x_0 \sqrt{2x_0} \delta(x_0 - x) \left[\left(-\frac{2}{\epsilon_c} \right) + \ln \frac{e^\gamma \mu^2}{4\pi \mu_c^2} \right] + \mathcal{O}(g_s \alpha_s^2), \quad (39)$$

where the pole is the collinear divergence with the index c . μ is the renormaliation scale related to the U.V. pole, and μ_c is that related to the collinear pole.

To find out the SGP contributions it is convenient to work with the light-cone gauge $n \cdot G = 0$. We consider a special class of diagrams which represent a part of one-loop corrections to those given in Fig.2. These diagrams are obtained from Fig.2. by adding a gluon. They are given in Fig.6. In the first four diagrams the gluon is emitted by the initial gluon and is absorbed by the final quark. In the last four diagrams the initial gluon goes across the cut represented by the broken line and emits a virtual gluon absorbed by the outgoing quark.

The contributions from Fig.6 contain a collinear divergence. In the first four diagrams, the divergence appears when the lowest gluon crossing the cut is collinear to the $+$ -direction. In the last four diagrams it appears when the gluon emitted by the outgoing quark is collinear. Because the contributions from Fig.6 are one-loop corrections to Fig.2, one may expect that the collinearly divergent parts of the contributions can be re-produced in the factorized form of the contributions from Fig.2. in Eq.(27), where one replaces $T_{q\pm}(x_1, x_2)$ with the corresponding one-loop $T_{q\pm}(x_1, x_2)$. As discussed in detail in [17], this is not the case, because the color factor here does not match. Even if one neglects the color factor, the divergences still can not be re-produced.

Analyzing the collinear divergences in the contributions of Fig.6, one finds that the collinear divergences should be factorized with $T_{q+}(x, x) = T_{q-}(x, x)$. Taking Fig.6a as an example, the added gluon is with momentum k_1 . If k_1 is collinear to the $+$ -direction, i.e., $k_1^\mu \sim (1, \lambda^2, \lambda, \lambda)$ with $\lambda \ll 1$, one can find that the gluon exchanged between the initial gluon and the initial antiquark is soft with the on-shell condition of the cut propagator. In fact, this gluon is a Glauber gluon with the momentum $\sim (\lambda^2, \lambda^2, \lambda, \lambda)$. Comparing Fig.6a with Fig.5, one can identify that the gluon crossing the cut in Fig.5 corresponds to the collinear gluon with k_1 in Fig.6a. If the collinear gluon is contained in $T_{q\pm}$, the Glauber gluon should be taken as the gluon entering hard scattering. Since it is a Glauber gluon with vanishing momentum, the divergent parts of Fig.6 should be factorized with $T_{q+}(x, x)$. This is the reason why the SGP contributions appear.

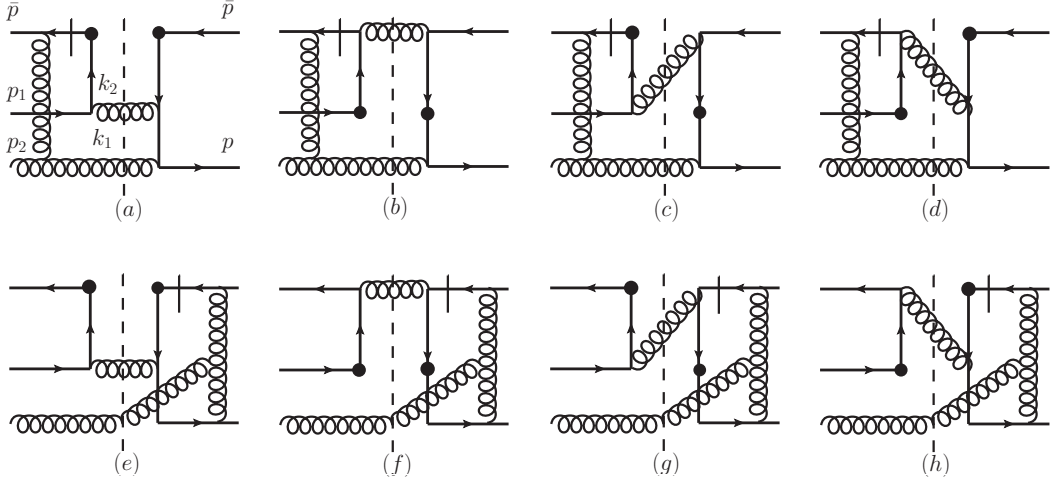


Figure 6: The diagrams for the amplitude $\bar{q} + [q + G] \rightarrow \gamma^* + X \rightarrow \bar{q} + q$ for SGP contributions. The black dots represent the insertion of electromagnetic current operator.

Performing the same analysis for Fig.6b, Fig.6c and Fig.6d in the case that the gluon crossing the cut is collinear, one will find that the gluon exchanged between the initial antiquark and the initial gluon is a Glauber gluon. For the last four diagrams the gluon emitted by the outgoing antiquark in the right part is a Glauber gluon, if the gluon emitted by the outgoing quark is collinear. Therefore, the collinear divergences in these diagrams are related to the Glauber gluon. It should be noted that only the diagrams in Fig.6 contain such a collinear divergence related to a Glauber gluon.

Before giving the results, the following facts should be pointed out. In Feynman gauge, one has to consider more diagrams which contain the collinear divergence, e.g., instead of that the collinear gluon is attached to the initial gluon in the left part of Fig.6, the gluon can also be attached to the initial antiquark. Such diagrams are finite in the light-cone gauge, at least for most cases studied here with an exception which will be discussed in Sect. 6. In the following we will work in the light-cone gauge $n \cdot G = 0$.

The contributions of Fig.6 contain an integration of a loop-momentum. It is easy to find the collinearly divergent part of the contributions by expanding the integrand in λ , where the collinear gluon has the momentum $\sim (1, \lambda^2, \lambda, \lambda)$. We find the collinearly divergent part of the contributions from Fig.6 as:

$$\mathcal{W}_T \Big|_{Fig.6} = C^{qg} \frac{e_q^2 g_s \alpha_s^2}{2\pi^2} \frac{N_c^2 - 1}{2N_c} \frac{\sqrt{2x_0}}{x_0} \left(-\frac{2}{\epsilon_c} \right) \cdot \left[\frac{x^2 - 2xx_0 - x_0^2 y}{(x_0 - x)^2 (1 - y)s} \delta(u) + \frac{x^2 + x_0^2 y^2}{(x_0 - x)(1 - y)} \delta'(u) \right],$$

$$\delta(u) = \delta(s(x_0 - x)(1 - y) - q_\perp^2). \quad (40)$$

In the above the pole in $\epsilon_c = 4 - d$ represents the collinear divergence. The δ -function from the on-shell condition of the intermediate gluon exchanged between quarks also depends on the loop momentum and needs to be expanded in λ . This results in the terms with the derivative of the δ -function. The last four diagrams do not contain terms with the derivative of the δ -function. With the result of $T_{q^+}(x, x)$ from the qg -contribution in Eq.(39) we can derive the factorized form:

$$\mathcal{W}_T \Big|_{Fig.6} = \frac{e_q^2 \alpha_s}{\pi^2 N_c q_\perp^2} \int_x^1 \frac{dy_1}{y_1} \int_y^1 \frac{dy_2}{y_2} f_{\bar{q}}(y_2) \delta(\hat{s}(1 - \xi_1)(1 - \xi_2) - q_\perp^2)$$

$$\begin{aligned} & \cdot \left[\tilde{\mathcal{S}}_{Gq}(\xi_1, \xi_2) \left(y_1 \frac{\partial T_{q+}(y_1, y_1)}{\partial y_1} \right) + \mathcal{S}_{Gq}(\xi_1, \xi_2) T_{q+}(y_1, y_1) \right], \\ \tilde{\mathcal{S}}_{Gq}(\xi_1, \xi_2) &= \frac{\xi_1^2 + \xi_2^2}{N_c(1 - \xi_2)}, \quad \mathcal{S}_{Gq}(\xi_1, \xi_2) = \frac{2\xi_1(1 - \xi_1)^2 - \xi_2^3 - \xi_1\xi_2(2 - \xi_1)}{N_c(1 - \xi_1)(1 - \xi_2)}. \end{aligned} \quad (41)$$

We note that the perturbative coefficient function here is at the same order of α_s as those of HP contributions because $T_{q+}(y_1, y_1)$ is at the order of $g_s\alpha_s$.

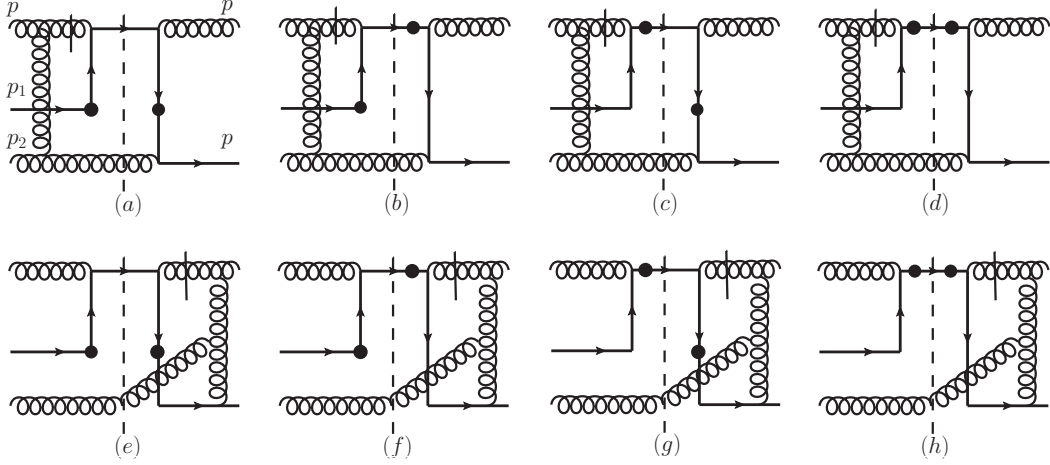


Figure 7: The diagrams for the amplitude $g + [q + G] \rightarrow \gamma^* + X \rightarrow g + q$ for SGP contributions. The black dots represent the insertion of electromagnetic current operator.

If we replace h_B with a gluon, one obtains similar diagrams from the SGP contributions from the gg -contributions. These diagrams are given in Fig.7. The collinearly divergent part of the contributions belong to the SGP contributions. We have calculated the collinear divergences in these diagrams in the light-cone gauge and in Feynman gauge. The same results are obtained. This corresponds to the situation with $T_{q\pm}(x, x)$ with Fig.5, only the same one diagrams in the two gauges gives the result in Eq.(39). From Fig.7 we have:

$$\begin{aligned} \mathcal{W}_T \Big|_{Fig.7} &= C^{gg} \frac{e_q^2 g_s \alpha_s^2 N_c^2}{4\pi^2} \sqrt{2x_0} \left[- \frac{s(1-y)(x^2 + 2xx_0(y-2) + 2x_0^2(y^2 - 2y + 2))}{q_\perp^2} \delta'(u) \right. \\ &\quad \left. + \frac{s(1-y)\delta(u)}{x_0(q_\perp^2)^2} \left((x_0 - x)(-xy + 2x + 3x_0y - 4x_0) - x_0^2 y(y^2 + (1-y)^2) \right) \right] \left(-\frac{2}{\epsilon_c} \right). \end{aligned} \quad (42)$$

With the result of $T_{q+}(x, x)$ from the gg -contribution in Eq.(39) we can derive the factorized form:

$$\begin{aligned} \mathcal{W}_T \Big|_{Fig.7} &= \frac{e_q^2 \alpha_s}{\pi^2 N_c q_\perp^2} \int_x^1 \frac{dy_1}{y_1} \int_y^1 \frac{dy_2}{y_2} f_g(y_2) \delta(\hat{s}(1 - \xi_1)(1 - \xi_2) - q_\perp^2) \\ &\quad \cdot \left[\tilde{\mathcal{S}}_{Gg}(\xi_1, \xi_2) \left(y_1 \frac{\partial T_{q+}(y_1, y_1)}{\partial y_1} \right) + \mathcal{S}_{Gg}(\xi_1, \xi_2) T_{q+}(y_1, y_1) \right], \\ \tilde{\mathcal{S}}_{Gg}(\xi_1, \xi_2) &= -\frac{N_c^2}{N_c^2 - 1} \left(\xi_1^2 + 2\xi_1(\xi_2 - 2) + 2(\xi_2^2 - 2\xi_2 + 2) \right), \end{aligned}$$

$$\mathcal{S}_{Gg}(\xi_1, \xi_2) = -\frac{N_c^2}{N_c^2 - 1} \left(-3\xi_1\xi_2 + 6\xi_1 - 2\xi_1^2 + 3\xi_2 - 4 - \frac{\xi_2(\xi_2^2 + (1 - \xi_2)^2)}{1 - \xi_1} \right). \quad (43)$$

The factorized results have also been also derived with the method of diagram expansion in [11].

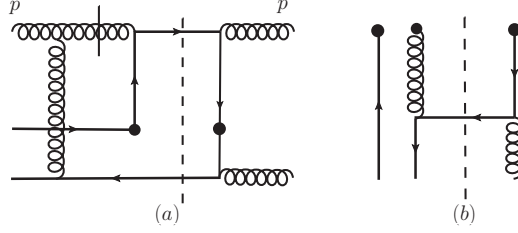


Figure 8: (a). The possible SGP-contributions from the $q\bar{q}$ -contributions. (b). The diagram for $T_{q\pm}(x, x)$ in the gauge $n \cdot G = 0$ from the $q\bar{q}$ -contributions. See the discussion in text.

In the case when h_B is replaced by a gluon, one can have the SGP contribution from the $q\bar{q}$ -contributions. An typical diagram is given in Fig.8. One can also obtain $T_{q\pm}(x, x)$ from the $q\bar{q}$ -contributions at this order. The diagram for it is given by Fig.8b. It is easy to find that the SGP contribution is included in the factorized form in Eq.(43).

Combining contributions of all flavors the SGP contributions can be factorized with the quark-gluon twist-3 matrix element as:

$$\begin{aligned} \mathcal{W}_T \Big|_{SGPF} &= \frac{\alpha_s}{\pi^2 N_c q_\perp^2} \int_x \frac{dy_1}{y_1} \int_y \frac{dy_2}{y_2} \delta(\hat{s}(1 - \xi_1)(1 - \xi_2) - q_\perp^2) \\ &\cdot \left[\tilde{\mathcal{S}}_{Gq}(\xi_1, \xi_2) \sum_{[q]} e_q^2 f_{\bar{q}}(y_2) \left(y_1 \frac{\partial T_{q+}(y_1, y_1)}{\partial y_1} \right) + \mathcal{S}_{Gq}(\xi_1, \xi_2) \sum_{[q]} e_q^2 f_{\bar{q}}(y_2) T_{q+}(y_1, y_1) \right. \\ &\left. + \tilde{\mathcal{S}}_{Gg}(\xi_1, \xi_2) \sum_{[q]} e_q^2 f_g(y_2) \left(y_1 \frac{\partial T_{q+}(y_1, y_1)}{\partial y_1} \right) + \mathcal{S}_{Gg}(\xi_1, \xi_2) \sum_{[q]} e_q^2 f_g(y_2) T_{q+}(y_1, y_1) \right]. \quad (44) \end{aligned}$$

The above results agree with those in [11, 8] derived with other method. Again, in the case of $q_\perp^2/Q^2 \ll 1$ this contribution takes a simplified form:

$$\begin{aligned} \mathcal{W}_T \Big|_{SGPF} &= \frac{\alpha_s}{\pi^2 N_c^2 (q_\perp^2)^2} \int_x \frac{dy_1}{y_1} \int_y \frac{dy_2}{y_2} \cdot \left[(1 + \xi_1^2) \delta(1 - \xi_2) \sum_{[q]} e_q^2 f_{\bar{q}}(y_2) \left(y_1 \frac{\partial T_{q+}(y_1, y_1)}{\partial y_1} \right) \right. \\ &+ \left(\frac{\delta(1 - \xi_2)}{(1 - \xi_1)_+} (2\xi_1^3 - 3\xi_1^2 - 1) - \frac{\delta(1 - \xi_1)}{(1 - \xi_2)_+} \xi_2 (1 + \xi_2^2) + 2\delta(1 - \xi_1) \delta(1 - \xi_2) \ln \frac{q_\perp^2}{Q^2} \right) \\ &\cdot \sum_{[q]} e_q^2 f_{\bar{q}}(y_2) T_{q+}(y_1, y_1) + \frac{N_c^3 \xi_2}{N_c^2 - 1} (\xi_2^2 + (1 - \xi_2)^2) \delta(1 - \xi_1) \sum_{[q]} e_q^2 f_g(y_2) T_{q+}(y_1, y_1) \left. \right] \\ &+ \dots \quad (45) \end{aligned}$$

where \dots stand for contributions suppressed by q_\perp^2/Q^2 .

5.2. The gg -Contributions

At the order we consider, there is no HP contribution from the gg -contributions. But, it is possible that there are leading SGP contributions from \mathcal{W}_T at one-loop level, similar to cases considered in the above. We consider first the gluonic twist-3 matrix elements in Eq.(11). These functions are zero at tree-level.

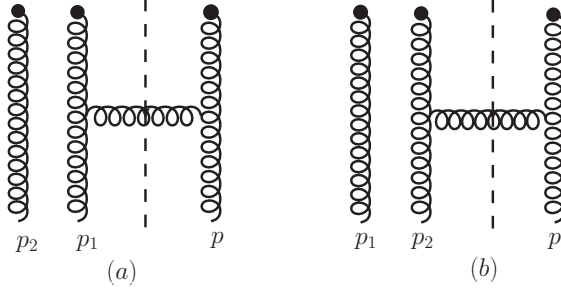


Figure 9: The diagrams for $G_{d1,f1}(x)$ and $G_{d2,f2}(x)$ in the light-cone gauge.

At one-loop level, the functions become nonzero. They receive nonzero contributions from the diagrams given in Fig.9 in the light-cone gauge. In Feynman gauge there are more diagrams. In this subsection we will work with the light-cone gauge. For the factorization studied below we only need to calculate Fig.9a and the corresponding diagrams for \mathcal{W}_T . The contributions from Fig.9b and the corresponding contributions to \mathcal{W}_T can be obtained from the permutation of the two initial gluons. We will only give results from Fig.9a and the corresponding results of \mathcal{W}_T . We obtain:

$$\begin{aligned}
G_{d1}(x) &= -\frac{g_s \alpha_s}{2\sqrt{2}} (N_c^2 - 4)(N_c^2 - 1) \delta(x - \bar{x}_0) \left[\left(-\frac{2}{\epsilon_c} \right) + \ln \frac{e^\gamma \mu^2}{4\pi \mu_c^2} \right] d_1, \\
G_{d2}(x) &= \frac{g_s \alpha_s}{4\sqrt{2}} (N_c^2 - 4)(N_c^2 - 1) \delta(x - \bar{x}_0) \left[\left(-\frac{2}{\epsilon_c} \right) + \ln \frac{e^\gamma \mu^2}{4\pi \mu_c^2} \right] d_2, \\
G_{f1}(x) &= \frac{g_s \alpha_s}{2\sqrt{2}} N_c^2 (N_c^2 - 1) \delta(x - \bar{x}_0) \left[\left(-\frac{2}{\epsilon_c} \right) + \ln \frac{e^\gamma \mu^2}{4\pi \mu_c^2} \right] f_1, \\
G_{f2}(x) &= -\frac{g_s \alpha_s}{4\sqrt{2}} N_c^2 (N_c^2 - 1) \delta(x - \bar{x}_0) \left[\left(-\frac{2}{\epsilon_c} \right) + \ln \frac{e^\gamma \mu^2}{4\pi \mu_c^2} \right] f_2,
\end{aligned} \tag{46}$$

with the parameters $d_{1,2}$ and $f_{1,2}$ related to \mathcal{F}_\pm^{gg} in Eq.(22) and \mathcal{D}_\pm^{gg} as:

$$\begin{aligned}
d_1 &= (1 - x_0) (x_0 \mathcal{D}_+^{gg} + \mathcal{D}_-^{gg}), & d_2 &= \mathcal{D}_+^{gg} + \mathcal{D}_-^{gg}, \\
f_1 &= (1 - x_0) (x_0 \mathcal{F}_+^{gg} + \mathcal{F}_-^{gg}), & f_2 &= \mathcal{D}_+^{gg} + \mathcal{D}_-^{gg}.
\end{aligned} \tag{47}$$

The corresponding contributions to \mathcal{W}_T are given by diagrams in Fig.10. The results for the color antisymmetric gluon state are:

$$\begin{aligned}
\mathcal{W}_T \Big|_{Fig.10} &= -\frac{e_q^2 g_s \alpha_s^2}{4\sqrt{2} \pi^2 N_c} \frac{N_c^2 (N_c^2 - 1)}{\bar{x}_0^3 (1 - y)} \left(-\frac{2}{\epsilon_c} \right) \left\{ \delta'(u) \left[2f_1 (2x^2 + 2x\bar{x}_0(y - 2) + \bar{x}_0^2(y - 2)^2) \right. \right. \\
&\quad \left. \left. - f_2 (4x^2 + 4x\bar{x}_0(y - 2) + \bar{x}_0^2(y^2 - 6y + 6)) \right] \right\}
\end{aligned}$$

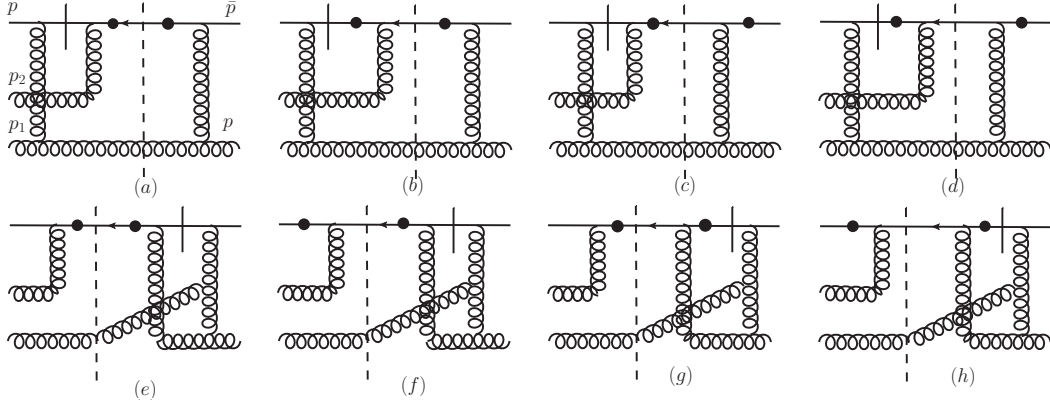


Figure 10: The diagrams for the amplitude $\bar{q} + (G + G) \rightarrow \gamma^* + X \rightarrow \bar{q} + G$ at one-loop for possible SGP contributions.

$$-\frac{\delta(u)}{s} \left[4f_1(2x + \bar{x}_0(y-2)) + 2f_2 \frac{x(5y-4) + \bar{x}_0(3y^2 - 7y + 4)}{1-y} \right] \Bigg\},$$

$$u = s(\bar{x}_0 - x)(1-y) - q_{\perp}^2. \quad (48)$$

Replacing the color factor $N_c^2(N_c^2 - 1)$ with $-(N_c^2 - 4)(N_c^2 - 1)$ and $f_{1,2}$ with $d_{1,2}$, respectively, one obtains \mathcal{W}_T from Fig.10 with the color structure of d^{abc} . With the results of the gluonic twist-3 matrix elements in Eq.(46) we can derive the factorized form from the SGP contribution from Fig.10 by combining all flavors as:

$$\begin{aligned} \mathcal{W}_T \Big|_{SGPG} &= \frac{\alpha_s}{\pi^2 N_c q_{\perp}^2} \int_x^1 \frac{dy_1}{y_1} \int_y^1 \frac{dy_2}{y_2} \delta(\hat{s}(1-\xi_1)(1-\xi_2) - q_{\perp}^2) \\ &\cdot \left\{ \sum_{i=1,2} \tilde{\mathcal{S}}_{Gi}(\xi_1, \xi_2) \sum_q e_q^2 \left[f_{\bar{q}}(y_2) \left(y_1 \frac{\partial G_{fi}(y_1, y_1)}{\partial y_1} + y_1 \frac{\partial G_{di}(y_1, y_1)}{\partial y_1} \right) \right. \right. \\ &+ f_q(y_2) \left. \left(y_1 \frac{\partial G_{fi}(y_1, y_1)}{\partial y_1} - y_1 \frac{\partial G_{di}(y_1, y_1)}{\partial y_1} \right) \right] \\ &+ \sum_{i=1,2} \mathcal{S}_{Gi}(\xi_1, \xi_2) \sum_q e_q^2 \left[f_{\bar{q}}(y_2) (G_{fi}(y_1, y_1) + G_{di}(y_1, y_1)) \right. \\ &+ f_q(y_2) (G_{fi}(y_1, y_1) - G_{di}(y_1, y_1)) \left. \right] \Bigg\} \quad (49) \end{aligned}$$

with the perturbative functions:

$$\begin{aligned} \tilde{\mathcal{S}}_{G1}(\xi_1, \xi_2) &= \frac{1-\xi_1}{1-\xi_2} \left(2\xi_1^2 + 2\xi_1(\xi_2 - 2) + (\xi_2 - 2)^2 \right), \\ \tilde{\mathcal{S}}_{G2}(\xi_1, \xi_2) &= \frac{1-\xi_1}{1-\xi_2} \left(4\xi_1^2 + 4\xi_1(\xi_2 - 2) + \xi_2^2 - 6\xi_2 + 6 \right), \\ \mathcal{S}_{G1}(\xi_1, \xi_2) &= -\frac{1-\xi_1}{1-\xi_2} \left(6\xi_1^2 + 4\xi_1(2\xi_2 - 3) + 3\xi_2^2 - 10\xi_2 + 8 \right), \\ \mathcal{S}_{G2}(\xi_1, \xi_2) &= -\frac{1-\xi_1}{1-\xi_2} \left(12\xi_1^2 + 6\xi_1(3\xi_2 - 4) + 7\xi_2^2 - 20\xi_2 + 14 \right). \quad (50) \end{aligned}$$

From the above results we can derive the result in the limit $q_\perp \rightarrow 0$ as:

$$\begin{aligned}
\mathcal{W}_T \Big|_{SGPG} &= \frac{\alpha_s}{\pi^2 N_c (q_\perp^2)^2} \int_x^1 \frac{dy_1}{y_1} \int_y^1 \frac{dy_2}{y_2} (1 - \xi_1) \delta(1 - \xi_2) \\
&\cdot \left\{ \sum_{i=1,2} \tilde{\mathcal{S}}_{\perp i}(\xi_1, \xi_2) \sum_q e_q^2 \left[f_{\bar{q}}(y_2) \left(y_1 \frac{\partial G_{fi}(y_1, y_1)}{\partial y_1} + y_1 \frac{\partial G_{di}(y_1, y_1)}{\partial y_1} \right) \right. \right. \\
&+ f_q(y_2) \left. \left(y_1 \frac{\partial G_{fi}(y_1, y_1)}{\partial y_1} - y_1 \frac{\partial G_{di}(y_1, y_1)}{\partial y_1} \right) \right] \\
&+ \sum_{i=1,2} \mathcal{S}_{\perp i}(\xi_1, \xi_2) \sum_q e_q^2 \left[f_{\bar{q}}(y_2) (G_{fi}(y_1, y_1) + G_{di}(y_1, y_1)) \right. \\
&+ \left. \left. f_q(y_2) (G_{fi}(y_1, y_1) - G_{di}(y_1, y_1)) \right) \right] \Big\} \tag{51}
\end{aligned}$$

with:

$$\begin{aligned}
\tilde{\mathcal{S}}_{\perp 1} &= 2\xi_1^2 - 2\xi_1 + 1, & \tilde{\mathcal{S}}_{\perp 2} &= 4\xi_1^2 - 4\xi_1 + 1, \\
\mathcal{S}_{\perp 1} &= -\left(6\xi_1^2 - 4\xi_1^2 + 1\right), & \mathcal{S}_{\perp 2} &= -\left(12\xi_1^2 - 6\xi_1^2 + 1\right). \tag{52}
\end{aligned}$$

The above the SGP contributions are leading contributions in the limit.

6. SQP-Contributions

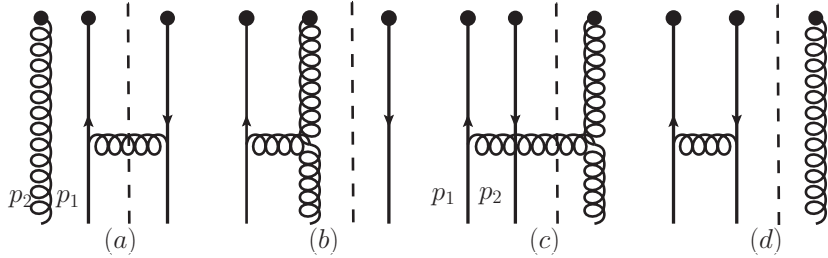


Figure 11: The diagrams for the twist-3 matrix elements with $x_2 = 0$ in the gauge $n \cdot G = 0$. The first two diagrams are for $x_1 > 0$ in qg -contributions. The later two diagrams are for $x_1 < 0$ in $q\bar{q}$ -contributions.

Similarly to the twist-3 matrix elements for SGP contributions, the twist-3 matrix elements for SQP contributions are zero at tree-level, because one can not define a quark state with zero momentum. Beyond tree-level, they can be nonzero. In the light-cone gauge $n \cdot G = 0$, one can find two possible diagrams at one-loop for the qg -contributions and the $q\bar{q}$ -contributions. They are given in Fig.11. It is easy to find that Fig.11b and Fig.11d will give zero contribution. We have for the qg -contributions from Fig.11a as:

$$\begin{aligned}
T_{q+}(x, 0) &= C^{qg} g_s \alpha_s \frac{N_c^2 - 1}{4N_c} \frac{x\sqrt{2x_0}}{x_0} \delta(x - \bar{x}_0) \left[-\left(\frac{2}{\epsilon_c}\right) + \ln \frac{e^\gamma \mu^2}{4\pi \mu_c^2} \right], \\
T_{q-}(x, 0) &= 0. \tag{53}
\end{aligned}$$

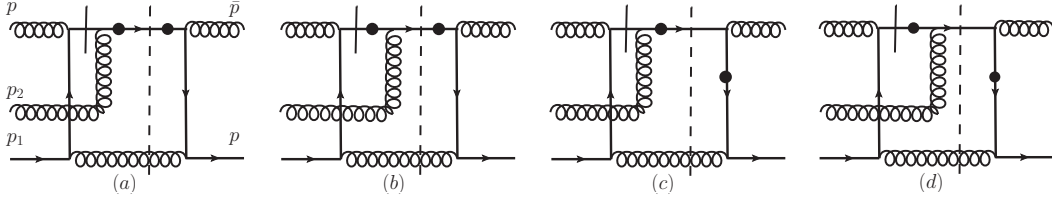


Figure 12: The diagrams in the $n \cdot G = 0$ gauge which give the soft fermion pole contributions to SSA.

We have for the $q\bar{q}$ -contributions from Fig.11c as:

$$\begin{aligned}
T_{q+}(x, 0) &= \left(\mathcal{C}_+^{q\bar{q}} - \mathcal{C}_-^{q\bar{q}} \right) g_s \alpha_s \delta(x + \bar{x}_0) \frac{N_c(N_c^2 - 1)}{4} \frac{\sqrt{2x_0\bar{x}_0}}{x_0} \left[- \left(\frac{2}{\epsilon_c} \right) + \ln \frac{e^\gamma \mu^2}{4\pi\mu_c^2} \right], \\
T_{q-}(x, 0) &= \left(\mathcal{C}_+^{q\bar{q}} + \mathcal{C}_-^{q\bar{q}} \right) g_s \alpha_s \delta(x + \bar{x}_0) \frac{N_c(N_c^2 - 1)}{4} \frac{\sqrt{2x_0\bar{x}_0}}{x_0} \bar{x}_0^2 \left[- \left(\frac{2}{\epsilon_c} \right) + \ln \frac{e^\gamma \mu^2}{4\pi\mu_c^2} \right]. \quad (54)
\end{aligned}$$

It is noted that in the above x is negative. It implies that an antiquark with the momentum fraction $-x$ enters a hard scattering.

The SQP contributions from the qg -contributions to \mathcal{W}_T are given by diagrams in Fig.12 in the gauge $n \cdot G = 0$. Following the analysis similar to that of Fig.6, one can see that the vertical quark line in the left part of diagrams carries the momentum k_q at the order of $k_q^\mu \sim (\lambda^2, \lambda^2, \lambda, \lambda)$, if the gluon at the bottom crossing the cut is collinear, i.e., its momentum scales like $(1, \lambda^2, \lambda, \lambda)$. Factorizing the collinear gluon into the corresponding twist-3 matrix elements, one can realize that in the left part of diagrams, there is a gluon combined with a soft quark entering the hard scattering. Therefore, the collinearly divergent contributions are SQP-contributions.

It is straightforward to find the divergent contributions from Fig.12:

$$\begin{aligned}
\mathcal{W}_T \Big|_{Fig.12} &= \mathcal{C}^{qg} \frac{e_q^2 g_s \alpha_s^2}{16\pi^2 N_c^2} \frac{\sqrt{2x_0} \delta(s(\bar{x}_0 - x)(1 - y) - q_\perp^2)}{q_\perp^2 (1 - x_0)} \left[\frac{(x(2x - 3(x_0 - 1)(y - 2)))}{1 - x_0} \right. \\
&\quad \left. + (1 - x_0)(y^2 - 5y + 5) - |\lambda_q|(x(y - 2) - (x_0 - 1)(y^2 - 3y + 3)) \right] \left(-\frac{2}{\epsilon_c} \right). \quad (55)
\end{aligned}$$

Again the quark-spin independent part should be factorized with the combination $T_{+q}(x, 0) + T_{-q}(x, 0)$, and the contribution with $|\lambda_q|$ should be factorized with $T_{+q}(x, 0) - T_{-q}(x, 0)$. With the results in Eq.(53) we have:

$$\begin{aligned}
\mathcal{W}_T \Big|_{Fig.12} &= \frac{e_q^2 \alpha_s}{2\pi^2 N_c q_\perp^2} \int_x^1 \frac{dy_1}{y_1} \int_y^1 \frac{dy_2}{y_2} f_g(y_2) \delta(\hat{s}(1 - \xi_1)(1 - \xi_2) - q_\perp^2) \\
&\quad \cdot \left[\mathcal{S}_{Qq+}(\xi_1, \xi_2) T_{q+}(y_1, 0) + \mathcal{S}_{Qq-}(\xi_1, \xi_2) T_{q-}(y_1, 0) \right], \\
\mathcal{S}_{Qq+}(\xi_1, \xi_2) &= \frac{1}{N_c^2 - 1} \left(\xi_1^2 + \xi_1 \xi_2 - 2\xi_1 - \xi_2 + 1 \right), \\
\mathcal{S}_{Qq-}(\xi_1, \xi_2) &= \frac{1}{N_c^2 - 1} \left((\xi_1 + \xi_2)^2 + 4(1 - \xi_1 - \xi_2) \right). \quad (56)
\end{aligned}$$

We turn to the $q\bar{q}$ -contributions. The contributions are given by diagrams in Fig.13 in the light-cone gauge. We need to find the collinear divergences related to the collinear gluon crossing the cut in these

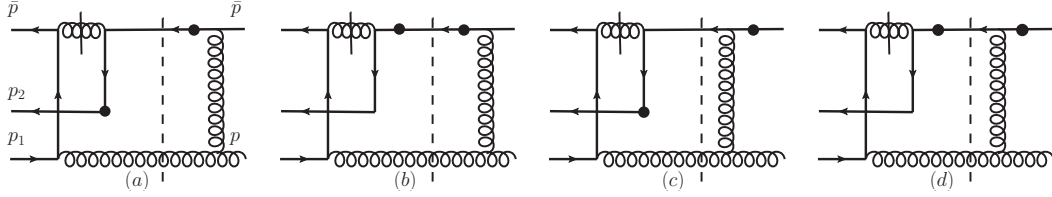


Figure 13: The diagrams in the gauge $n \cdot G = 0$ for the amplitude $\bar{q} + (q + \bar{q}) \rightarrow \gamma^* + X \rightarrow \bar{q} + G$ at one-loop for possible SFP contributions.

diagrams. But, a direct calculation of the collinear divergences in these diagrams will give wrong results. This is the exception mentioned in Sect.5.1 before Eq.(40). We will explain this with Fig.13a as an example. In this diagram, the collinear divergence appears when the gluon attached to the initial quark is collinear to the $+$ -direction. Instead of attaching the collinear gluon to the initial quark, it can also be attached to other places. There are two examples given by the diagrams in Fig.14.

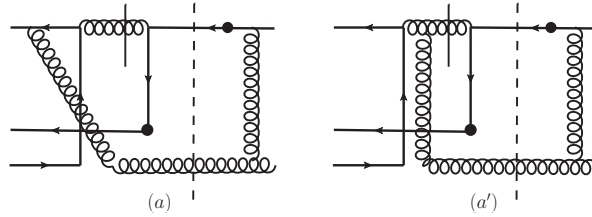


Figure 14: The diagrams obtained from Fig.13a by changing the attachment of the collinear gluon.

As discussed in Sect.5.1., one may expect that these two diagrams in Fig.14 do not have the discussed collinear divergence in the gauge $n \cdot G = 0$. Because of the structure of the color factor, Fig.14a' is always zero. But, through an explicit calculation one finds that Fig.14a also contains the collinear divergence. Similarly to Fig.13a, we can obtain the corresponding diagram Fig.14b, Fig.14c and Fig.14d from Fig.13b, Fig.13c and Fig.13d, respectively. These diagrams are not drawn in Fig.14. They also contain collinear divergences. If the divergences survive in the end results, it implies that the factorization is broken. This needs to be carefully examined.

We use k to denote the momentum carried by the gluon crossing the broken line. If the gluon is collinear, k has the pattern:

$$k^\mu \sim (1, \lambda^2, \lambda, \lambda), \quad \lambda \ll 1. \quad (57)$$

We use k_g to denote the momentum carried by the gluon propagator with the short bar. The propagator has three terms in the light-cone gauge:

$$\pi \delta(k_g^2) \left[-g^{\mu\nu} + \frac{n^\nu k_g^\mu}{n \cdot k_g} + \frac{n^\mu k_g^\nu}{n \cdot k_g} \right]. \quad (58)$$

In the above μ is the index contracted with that in the vertex left to the short bar, and ν is contracted with that in the vertex right to the short bar. The first term will not give collinear divergence in Fig.14a. But, the second and third term will give collinear divergences with the collinear power-counting, because

the denominator of the terms is at order of λ^2 , i.e., $n \cdot k_q \sim \lambda^2$ derived from the on-shell condition $\delta(k_q^2)$ with Eq.(57).

The propagator in Eq.(58) also appear in Fig.13a. The second term gives no contribution because of $\bar{v}(\bar{p})n \cdot \gamma = 0$. The contributions from the first- and third term contain the collinear divergences. It is easy to show that the divergence from the third term is canceled by that from the first term in Fig.14a. This also happens for other diagrams in Fig.13 in a similar way. Through explicit calculation we find that the divergence introduced by the second term in Fig.14a and Fig.14b are canceled by that in Fig.14c and Fig.14d, respectively. Therefore, only the collinear divergences in Fig.13 introduced by the first term in Eq.(58) survive at the end, if we include all diagrams from Fig.13 and Fig.14 in the gauge $n \cdot G = 0$. The diagrams in the light-cone gauge by changing the attachment of the collinear gluon in the right part of diagrams in Fig.13 do not contain collinear divergences. This has the implication for using the diagram expansion in the light-cone gauge, where one will have the uncanceled divergences from the cut gluon-propagator. With the method in Feynman gauge one will not have such divergences.

From the above discussion the correct result is to obtain by taking only the first term in Eq.(58) to calculate the diagrams in Fig.13, or by taking all in Eq.(58) to calculate all diagrams in Fig.13 and Fig.14. We obtain:

$$\mathcal{W}_T \Big|_{Fig.13} = -\frac{e_q^2 g_s \alpha_s^2}{8\pi^2} \frac{N_c^2 - 1}{N_c} \left(-\frac{2}{\epsilon_c} \right) \frac{\sqrt{2x_0 \bar{x}_0}}{x_0 \bar{x}_0 q_\perp^2} \delta(s(\bar{x}_0 - x)(1 - y) - q_\perp^2) \left[\frac{(1 - y)\bar{x}_0 - x}{\bar{x}_0^2} (\bar{x}_0 - x) (C_+^{q\bar{q}} - C_-^{q\bar{q}}) + (x + \bar{x}_0 y - 2\bar{x}_0)^2 (C_+^{q\bar{q}} + C_-^{q\bar{q}}) \right]. \quad (59)$$

With the results of relevant twist-3 matrix element in Eq.(54) one can derive the following factorized form:

$$\begin{aligned} \mathcal{W}_T \Big|_{Fig.13} &= \frac{e_q^2 \alpha_s}{\pi^2 N_c q_\perp^2} \int_x^1 \frac{dy_1}{y_1} \int_y^1 \frac{dy_2}{y_2} \bar{q}(y_2) \delta(\hat{s}(1 - \xi_1)(1 - \xi_2) - q_\perp^2) \\ &\quad \cdot \left[\mathcal{S}_{Qq\bar{q}+}(\xi_1, \xi_2) T_{q+}(-y_1, 0) + \mathcal{S}_{Qq\bar{q}-}(\xi_1, \xi_2) T_{q-}(-y_1, 0) \right], \\ \mathcal{S}_{Qq\bar{q}+}(\xi_1, \xi_2) &= -\frac{1 - \xi_1}{2N_c} (1 - \xi_1 - \xi_2), \quad \mathcal{S}_{Qq\bar{q}-}(\xi_1, \xi_2) = -\frac{(2 - \xi_1 - \xi_2)^2}{2N_c}. \end{aligned} \quad (60)$$

For the gg -contributions there are also a SQP contribution, where one can obtain $T_{q\pm}(x, 0)$ from the gg -contributions at one-loop. The SQP contribution in \mathcal{W}_T is obtained by replacing h_B with a gluon at one-loop. This contribution is in fact contained in the factorized form in Eq.(56). This is similar to the case in $q\bar{q}$ -contributions for the SGP-contributions with Fig.8 discussed in Sect.5.1.

Combining all flavors we obtain then the factorized SQP contributions as:

$$\begin{aligned} \mathcal{W}_T \Big|_{SQP} &= \frac{\alpha_s}{\pi^2 N_c q_\perp^2} \int_x^1 \frac{dy_1}{y_1} \int_y^1 \frac{dy_2}{y_2} \delta(\hat{s}(1 - \xi_1)(1 - \xi_2) - q_\perp^2) \\ &\quad \cdot \left[\mathcal{S}_{Qq+}(\xi_1, \xi_2) \sum_{[q]} e_q^2 f_g(y_2) T_{q+}(y_1, 0) + \mathcal{S}_{Qq-}(\xi_1, \xi_2) \sum_{[q]} e_q^2 f_g(y_2) T_{q-}(y_1, 0) \right. \\ &\quad \left. + \mathcal{S}_{Qq\bar{q}+}(\xi_1, \xi_2) \sum_{[q]} e_q^2 f_{\bar{q}}(y_2) T_{q+}(-y_1, 0) + \mathcal{S}_{Qq\bar{q}-}(\xi_1, \xi_2) \sum_{[q]} f_{\bar{q}}(y_2) T_{q-}(-y_1, 0) \right]. \end{aligned} \quad (61)$$

In comparison with the existing results in [8] derived with the method of diagram expansion our results of SQP contributions are different. The difference is of an overall factor of -2 . We note that the SQP

contribution is proportional to q_{\perp}^{-2} in the limit $q_{\perp}^2 \rightarrow 0$. Hence, it is not a leading contribution in the limit $q_{\perp}^2/Q^2 \ll 1$.

7. Summary

We have studied the collinear factorization of SSA in Drell-Yan processes. To derive all perturbative coefficient functions at leading order of α_s in the factorization, we have studied the scattering with multi-parton states, in which the helicity of the states are flipped. SSA in such a scattering is nonzero. This is in contrast to the scattering with a transversely polarized single quark. In this case SSA is always zero because of the helicity conservation of QCD for massless quarks.

We have calculated SSA in the multi-parton scattering processes and the relevant twist-3 matrix elements of multi-parton states. By using the results from our calculation SSA has been factorized as convolutions of twist-3 matrix elements of the polarized hadron, parton distribution functions of the unpolarized hadron and perturbative coefficient functions. All perturbative coefficient functions of these contributions are derived here at the leading order of α_s . In the factorization there are HP-, SGP- and SFP-contributions. From our results, we find that SSA at tree-level is factorized as the HP contributions. But the SGP- and SFP- contributions are from a class of one-loop contributions to SSA. These one-loop contributions contain collinear divergences and they can only be factorized with the soft-pole twist-3 matrix elements in which one of the active patrons carries zero momentum. These soft-pole twist-3 matrix elements are zero at tree-level but nonzero at one-loop. This results in that the perturbative coefficient functions of SGP- and SQP contributions are at the same order as those of HP contributions. Hence, in the collinear factorization there is a nontrivial order-mixing. Such an order-mixing does not happen in the factorization only involving twist-2 operators.

It is interesting to note that at one-loop SSA contains divergences caused by exchanges of a Glauber gluon, as discussed in Sect.5. The divergences are factorized with the soft-gluon-pole matrix elements. This is in contrast to the factorization of unpolarized cross-section only with twist-2 operators, where it is well known that the divergences from exchanges of Glauber gluons are canceled[38, 39, 40]. In the case of SSA studied here with twist-3 operators, such divergences are not canceled and need to be factorized. This will have some implications for the study of factorizations in the framework of soft collinear effective theories of QCD[41].

Our results for the collinear factorization of SSA in Drell-Yan processes agree with those derived with the method of diagram expansion, except the SQP contributions studied in Sect.6. Comparing the method of the diagram expansion, we believe that it has advantages to use our method with multi-parton states for analyzing factorizations of SSA and for calculating higher order corrections, because the involved calculations are of standard scattering amplitudes. The approach we have taken here provides another way to derive the collinear factorization of SSA in various processes. It will be useful to solve the discrepancy between results for SSA in [42], where the momentum of a lepton in Drell-Yan processes is measured. It will also be useful for solving the discrepancy of evolutions of twist-3 matrix elements derived in [43, 44, 45]. We leave these for future work.

Note Added: During the preparation of the paper the results of the SGP-contributions with gluonic twist-3 matrix elements is reported in [46]. The results there agree with ours in Sect. 5.2..

Acknowledgments

This work is supported by National Nature Science Foundation of P.R. China(No. 10975169,11021092). The work of H.Z. Sang is supported by the Fundamental Research Funds for the Central Universities(WM1114025) and by National Nature Science Foundation of P.R. China(No. 11147168).

References

- [1] U. D'Alesio and F. Murgia, *Prog. Part. Nucl. Phys.***61** (2008) 394, e-Print: arXiv:0712.4328 [hep-ph].
- [2] G.L. Kane, J. Pumplin and W. Repko, *Phys. Rev. Lett.* **41** (1978) 1689.
- [3] W.G.D. Dharmaratna and G.R. Goldstein, *Phys. Rev. D*41 (1990) 1731, W. Bernreuther, J.P. Ma and T. Schroder, *Phys. Lett. B*297 (1992) 318, W. Bernreuther, J.P. Ma and B.H.J. McKellar, *Phys. Rev. D*51 (1995) 2475.
- [4] J.W. Qiu and G. Sterman, *Phys. Rev. Lett* **67** (1991) 2264, *Nucl. Phys. B*378 (1992) 52, *Phys. Rev. D*59 (1998) 014004.
- [5] A.V. Efremov and O.V. Teryaev, *Sov. J. Nucl. Phys.* **36** 1982 142, *Phys. Lett. B*150 (1985) 383.
- [6] Y. Kanazawa and Y. Koike, *Phys. Lett. B*478 (2000) 121, *Phys.Rev. D*64 (2001) 034019.
- [7] H. Eguchi, Y. Koike and K. Tanaka, *Nucl. Phys. B*752 (2006) 1, e-Print: hep-ph/0604003, *Nucl. Phys. B*763 (2007) 198, e-Print: hep-ph/0610314, Y. Koike and K. Tanaka, *Phys. Rev. D*76 (2007) 011502, e-Print: hep-ph/0703169, Y. Koike and T. Tomita, *Phys. Lett. B*675 (2009) 181, e-Print: arXiv:0903.1923 [hep-ph], H. Beppu, Y. Koike, K. Tanaka and S. Yoshida, *Phys. Rev. D*82 (2010) 054005, e-Print: arXiv:1007.2034 [hep-ph].
- [8] K. Kanazawa and Y. Koike, *Phys. Lett. B*701 (2011) 576, e-Print: arXiv:1105.1036 [hep-ph].
- [9] J.W. Qiu, W. Vogelsang and F. Yuan, *Phys. Lett. B*650 (2007) 373, e-Print: arXiv:0704.1153, *Phys. Rev. D*76 (2007) 074029, e-Print: arXiv:0706.1196, Z.-B Kang and J.W Qiu, *Phys.Rev. D*78 (2008) 034005, e-Print: arXiv:0806.1970.
- [10] F. Yuan, *Phys. Rev. D*78 (2008) 014024, e-Print: arXiv:0801.4357, C.J. Bomhof, P.J. Mulders, W. Vogelsang and F. Yuan, *Phys.Rev.D*75 (2007) 074019, e-Print: hep-ph/0701277, C. Kouvaris, J.W. Qiu, W. Vogelsang and F. Yuan, *Phys.Rev.D*74 (2006) 114013, e-Print: hep-ph/0609238, F. Yuan and J. Zhou, *Phys. Lett. B*668 (2008) 216, e-Print: arXiv:0806.1932.
- [11] X.D. Ji, J.W. Qiu, W. Vogelsang and F. Yuan, *Phys. Rev. Lett.* **97** (2006) 082002, e-Print: hep-ph/0602239, *Phys. Rev. D*73 (2006) 094017, e-Print: hep-ph/0604023.
- [12] X.D. Ji, J.W. Qiu, W. Vogelsang and F. Yuan, *Phys. Lett. B*638 (2006) 178, e-Print: hep-ph/0604128.
- [13] Y. Koike, W. Vogelsang and F. Yuan, *Phys. Lett. B*659 (2008) 878, e-Print: arXiv:0711.0636.
- [14] H.G. Cao, J.P. Ma and H.Z. Sang, *Commun. Theor. Phys.* **53** (2010) 313-324, e-Print: arXiv:0901.2966 [hep-ph].

- [15] J.P. Ma and H.Z. Sang, JHEP 1104:062, 2011, e-Print: arXiv:1102.2679 [hep-ph].
- [16] J.P. Ma and H.Z. Sang, JHEP 0811:090,2008, e-Print: arXiv:0809.4811 [hep-ph].
- [17] J.P. Ma and H.Z. Sang, Phys. Lett. B676 (2009) 74, e-Print: arXiv:0811.0224 [hep-ph].
- [18] J.W. Qiu and G.F. Sterman, Nucl. Phys. B353 (1991) 105, Nucl. Phys. B353: (1991) 137.
- [19] J.W. Qiu, Phys. Rev. D42 (1990) 30.
- [20] X.D. Ji, Phys. Lett. B289 (1992) 137.
- [21] D. Sivers, Phys. Rev. D41 (1990) 83, Phys. Rev. D43 (1991) 261.
- [22] J. C. Collins, Nucl. Phys. B396 (1993) 161, Phys. Lett. B536 (2002) 43.
- [23] J.C. Collins and D.E. Soper, Nucl. Phys. B193 (1981) 381, Nucl. Phys. B213 (1983) 545(E), Nucl. Phys. B197 (1982) 446, Nucl. Phys. B194 (1982) 445.
- [24] J.C. Collins, D.E. Soper and G. Sterman, Nucl. Phys. B250 (1985) 199.
- [25] X.D. Ji, J.P. Ma and F. Yuan, Phys. Rev. D71 (2005) 034005, Phys. Lett. B597 (2004) 299.
- [26] X.D. Ji, J.P. Ma and F. Yuan, JHEP 0507:020,2005, hep-ph/0503015
- [27] J.C. Collins and A. Metz, Phys. Rev. Lett. **93** 252001.
- [28] J. C. Collins, Nucl. Phys. B396 (1993) 161, Phys. Lett. B536 (2002) 43.
- [29] S.J. Brodsky et al., Phys. Rev. D65 (2002) 114025.
- [30] X.D. Ji and F. Yuan, Phys. Lett. B543 (2002) 66, A.V. Belitsky, X.D. Ji and F. Yuan, Nucl. Phys. B656 (2003) 165.
- [31] D. Boer and P. J. Mulders, Phys. Rev. D57 (1998) 5780, P.J. Mulders and R.D. Tangerman, Nucl. Phys. B461 (1996) 197, Nucl. Phys. B484 (1997) 538(E).
- [32] D. Boer, P.J. Mulders and F. Pijlman, Nucl. Phys. B667 (2003) 201.
- [33] M. Anselmino, M. Boglione and F. Murgia, Phys. Lett. B362 (1995) 164; M. Anselmino and F. Murgia, Phys. Lett. B442 (1998) 470; M. Anselmino and F. Murgia, Phys. Lett. B483 (2000) 74; M. Anselmino, U. D'Alesio and F. Murgia, Phys.Rev. D67 (2003) 074010, U. D'Alesio and F. Murgia, Phys. Rev. D70 (2004) 074009, Anselmino, *et al.*, Phys. Rev. D73 (2006) 014020.
- [34] P. J. Mulders and R. D. Tangerman, Nucl. Phys. B461 (1996) 197 [Erratum-ibid. B484 (1997) 538]; D. Boer, Phys. Rev. D60 (1999) 014012.
- [35] E. De Sanctis, W.D. Nowak and K.A. Oganesian, Phys. Lett. B483 (2000) 69; V.A. Korotkov, W. D. Nowak and K.A. Oganesian, Eur. Phys. J. C18 (2001) 639; K.A. Oganesian, N.Bianchi, E. De Sanctis and W.D. Nowak, Nucl. Phys. A689 (2001) 784;
- [36] A.V. Efremov, K. Goeke, M. V. Polyakov and D. Urbano, Phys. Lett. B478 (2000) 94; A.V. Efremov, K. Goeke and P. Schweitzer, Eur. Phys. J. C24 (2002) 407, Nucl. Phys. A711 (2002) 84, Phys. Lett. B522 (2001) 37, Phys. Lett. B544 (2002) 389(E), Phys. Lett. B568 (2003) 63.

- [37] B. Q. Ma, I. Schmidt and J. J. Yang, Phys. Rev. D66 (2002) 094001, Phys. Rev. D65 (2002) 034010.
- [38] G.T. Bodwin, S.J. Brodsky and G.P. Lepage, Phys. Rev. Lett. **47** (1981) 1799, G.T. Bodwin, Phys. Rev. D31 (1985) 2616, G.T. Bodwin, S.J. Brodsky and G.P. Lepage, Phys. Rev. D39 (1989) 3287, J.C. Collins and D.E. Soper, Nucl. Phys. B185 (1981) 172.
- [39] J.C. Collins, D.E. Soper and G. Sterman, Phys. Lett. B109 (1982) 388, Phys. Lett. B134 (1984) 263.
- [40] J.C. Collins, D.E. Soper and G. Sterman, Nucl. Phys. B261 (1985) 104, Nucl. Phys. B308 (1988) 833.
- [41] F. Liu and J.P. Ma, e-Print: arXiv:0802.2973 [hep-ph].
- [42] N. Hammon, O. Teryaev and A. Schäfer, Phys. Lett. B390 (1997) 409, arXiv: hep-ph/9611369, D. Boer, P.J. Mulders and O.V. Teryaev, Phys. Rev. D57 (1998) 3057, arXiv: hep-ph/970223, D. Boer and P.J. Mulders, Nucl. Phys. B569 (1990) 505, arXiv: hep-ph/9906223, D. Boer and J.W. Qiu, Phys. Rev. D65 (2002) 034008, arXiv: hep-ph/0108179, J.P. Ma and Q. Wang, Eur. Phys. J. C37 (2004) 293-298, arXiv: hep-ph/0310245, I.V. Anikin and O.V. Teryaev, Phys. Lett. B690 (2010) 519, arXiv: 1003.1482[hep-ph], J. Zhou and A. Metz, arXiv:1011.5871 [hep-ph].
- [43] Z.-B. Kang and J.-W. Qiu, Phys. Rev. D79:016003,2009, e-Print: arXiv:0811.3101 [hep-ph].
- [44] V.M. Braun, A.N. Manashov and B. Pirnay, Phys. Rev. D80 (2009) 114002, e-Print: arXiv:0909.3410 [hep-ph].
- [45] J. Zhou, F. Yuan and Z.T. Liang, Phys. Rev. D79 (2009) 114022, arXiv:0812.4484[hep-ph].
- [46] Y. Koike and S.Yoshida, e-Print: arXiv:1110.6496 [hep-ph].